ปฏิกิริยาไฮโดรจิเนชันในวัฏภาคของเหลวโดยตัวเร่งปฏิกิริยาแพลเลเดียมบนซิลิกาที่เตรียมโดยวิธีโซล-เจล

นางสาวกรรณิการ์ แผ่นดินทอง

LIQUID-PHASE HYDROGENATION OVER PALLADIUM CATALYSTS SUPPORTED ON SOL-GEL-DERIVED SILICA

Miss Kunnika Phandinthong

A Thesis Submitted in Partial Fulfillment of the Requirements

for the Degree of Master of Engineering Program in Chemical Engineering

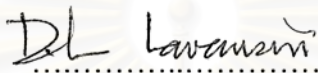Department of Chemical Engineering

Faculty of Engineering

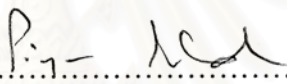Chulalongkorn University

Academic Year 2005

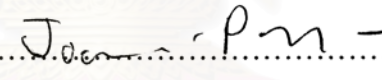|	
Thesis Title	LIQUID-PHASE HYDROGENATION OVER PALLADIUM CATALYSTS SUPPORTED ON SOL-GEL-DERIVED SILICA
By	Miss Kunnika Phandinthong
Field of Study	Chemical Engineering
Thesis Advisor	Assistant Professor Joongjai Panpranot, Ph.D.
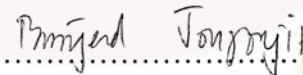
Accepted by the Faculty of Engineering, Chulalongkorn University in Partial Fulfillment of the Requirements for the Master's Degree
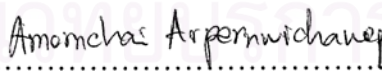
.... Dean of the Faculty of Engineering

(Professor Direk Lavansiri, Ph.D.)

THESIS COMMITTEE

.... Chairman

(Professor Piyasan Praserthdam, Dr.Ing.)

.... Thesis Advisor

(Assistant Professor Joongjai Panpranot, Ph.D.)

.... Member

(Assistant Professor Bunjerd Jongsomjit, Ph.D.)

.... Member

(Amornchai Arpornwichanop, D.Eng.)

กรรณิการ์ แผ่นดินทอง: ปฏิกิริยาไฮโดรจิเนชันในวัฏภาคของเหลวโดยตัวเร่งปฏิกิริยา
แพลเลเดียมบนซิลิกาที่เตรียมโดยวิธีโซล-เจล (LIQUID-PHASE HYDROGENATION
OVER PALLADIUM CATALYSTS SUPPORTED ON SOL-GEL-DERIVED SILICA)
อ. ที่ปรึกษา: ผ.ศ. ดร. จุงใจ ปั้นประณต, 85 หน้า. ISBN: 974-17-3933-8

วิทยานิพนธ์นี้ศึกษาเปรียบเทียบลักษณะเฉพาะและคุณสมบัติการเร่งปฏิกิริยาของตัวเร่ง
ปฏิกิริยาแพลเลเดียมบนตัวรองรับซิลิกาชนิดต่างๆ ในเทอมของความว่องไวของการเกิดปฏิกิริยา
ไฮโดรจิเนชันในวัฏภาคของเหลวของฟีนิลอะเซทิลีน การเลือกเกิดของสไตรีน และการเสื่อมสภาพ
ของตัวเร่งปฏิกิริยา โดยที่ตัวเร่งปฏิกิริยาจะถูกเตรียมโดยใช้ 2 วิธีคือ การแลกเปลี่ยนประจุและการ
เคลือบฝัง พบว่าการเตรียมตัวเร่งปฏิกิริยาด้วยวิธีแลกเปลี่ยนประจุโดยใช้ซิลิกาที่เตรียมด้วยวิธี
โซล-เจล เกิดสารประกอบแพลเลเดียมซิลิไซด์ จากการศึกษาคุณสมบัติการเร่งปฏิกิริยาและการ
เลือกเกิดของตัวเร่งปฏิกิริยาพบว่า ตัวเร่งปฏิกิริยาแพลเลเดียมที่อยู่บนตัวรองรับซิลิกาที่เตรียมด้วย
วิธีโซล-เจลจะให้ประสิทธิภาพดีกว่าตัวเร่งปฏิกิริยาที่อยู่บนตัวรองรับซิลิกา (commercial) และ
ตัวเร่งปฏิกิริยวแพลเลเดียมซิลิไซด์มีประสิทธิภาพสูงสุด นอกจากนี้ได้ศึกษาผลของตัวทำละลายที่
มีต่อปฏิกิริยาไฮโดรจิเนชันในวัฏภาคของเหลว โดยใช้ไซโคลเฮกซีนเป็นสารตั้งต้น ตัวทำละลาย
อินทรีย์ที่นำมาใช้ในการศึกษาคือ เบนซีน เฮปทานอล นอร์มอลเมทิลไพโรริโดน (NMP) รวมทั้ง
คาร์บอนไดออกไซด์ที่สภาวะเหนือวิกฤต (supercritical CO_2) ในกรณีที่ใช้ตัวทำละลายอินทรีย์
ความว่องไวในการเกิดปฏิกิริยาจะขึ้นกับความมีขั้วของตัวทำละลาย โดยตัวทำละลายที่มีความมี
ขั้วสูงจะมีความว่องไวในการเกิดปฏิกิริยาต่ำ และการใช้คาร์บอนไดออกไซด์ที่สภาวะเหนือวิกฤต
(supercritical CO_2) จะเพิ่มความสามารถในการละลายของก๊าซไฮโดรเจนในสารตั้งต้นเป็นผลให้
ความว่องไวในการเกิดปฏิกิริยาเพิ่มขึ้น การเสื่อมสภาพของตัวเร่งปฏิกิริยาเนื่องจากการรวมตัวกัน
และการชะล้างของแพลเลเดียมมีค่าใกล้เคียงกันทั้งในกรณีของตัวทำละลายอินทรีย์และ
คาร์บอนไดออกไซด์ที่สภาวะเหนือวิกฤต (supercritical CO_2)

ภาควิชา..............วิศวกรรมเคมี.......... ลายมือชื่อนิสิต......กรรณิการ์ แผ่นดินทอง.....
สาขาวิชา............วิศวกรรมเคมี.......... ลายมือชื่ออาจารย์ที่ปรึกษา......................
ปีการศึกษา..........2548...................

KUNNIKA PHANDINTHONG: LIQUID-PHASE HYDROGENATION OVER PALLADIUM CATALYSTS SUPPORTED ON SOL-GEL-DERIVED SILICA THESIS ADVISOR: ASST. PROF. JOONGJAI PANPRANOT Ph.D., 85 pp. ISBN: 974-17-3933-8

The characteristic and catalytic properties of different silica supported palladium catalysts were investigated and compared in term of catalytic activities for liquid-phase hydrogenation of phenylacetylene, styrene selectivities and catalyst deactivation. Catalysts were prepared by two different methods, ion-exchange and impregnation. It was found that the sol-gel derived silica supported palladim catalyst prepared by ion-exchange method formed palladium silicide. From catalytic activities and selectivities study, the palladium catalysts supported on the sol-gel derived silica prepared by both methods exhibited better performances compared to those supported on commercial silica with the palladium silicide showed the best performance. Moreover, the effects of solvents on catalytic activity of Pd/SiO_2 catalysts in liquid-phase hydrogenation were investigated using cyclohexene as a model reactant. The solvents used were benzene, heptanol, n-methyl pyrolidone (NMP) and supercritical CO_2. In the cases of using organic solvents, the hydrogenation rates depended on polarity of the solvents in which the reaction rates in high polar solvents were lower. The use of high pressure CO_2 can probably enhance H_2 solubility in the substrate resulting in a higher hydrogenation activity. However, metal sintering and leaching in the presence of high pressure CO_2 were comparable to those in organic solvents.

Department .....Chemical Engineering...... Student's signature Kunnika Phandinthong

Field of Study...Chemical Engineering..... Advisor's signature .....

Academic year ....2005...............

ACKNOWLEDGEMENTS

CONTENTS

CHAPTER

LIST OF TABLES

LIST OF FIGURES

FIGURE **Page**

CHAPTER I

INTRODUCTION

1.1 Rationale

Catalytic hydrogenation is one of the most useful, versatile, and environmentally acceptable reaction routes available for organic syntheses because the scope of the reaction type is very broad and many functional groups can be hydrogenated with high selectivity and high conversion. A large number of these reactions are carried out in liquid phase using batch type slurry processes.

Hydrogenation reactions are mostly catalyzed by noble metals or group VIII transition metals. The major advantages of noble metal catalysts are their relatively high activity, mild process conditions, easy separation, and better handling properties. Noble metals such as, Pt, Pd, Rh, and Ru are particularly effective in hydrogenation processes because they adsorb hydrogen with dissociation and the bonding is not too strong. The ability of the metal to dissociate the hydrogen molecules partly determines the activity of the catalyst. The hydrogenation activity generally decreases in the following sequence: Pd > Rh > Pt > Ru. Catalysis by noble metals is usually achieved via the high dispersion of low loading metals on an appropriate support. The supports are usually of relatively inexpensive oxide such as alumina, silica, and titania.

Several factors affecting the performance of noble metal catalysts in liquid phase hydrogenation have been extensively investigated. Typically, the factors can be classified into (i) the role of the liquid phase composition (substrate structure, solvent effect, etc.), (ii) the effect of catalysts (active sites composition and morphology, support effects, SMSI, modifiers, etc.), and (iii) the effect of reaction conditions (temperature, pressure, etc.) on reaction kinetics. A solvent in liquid-phase heterogeneous catalytic systems can have a significant effect on kinetic behavior. Mass transfer limitation is an obvious one,

especially pore diffusion, but other possibilities such as solvent properties and competitive adsorption of the solvent for sites may also occur.

The important problem in catalytic liquid phase hydrogenation is the activity and selectivity decay due to catalyst deactivation. The main causes of catalyst deactivation in liquid phase hydrogenation are

1. Sintering of metal particles and coalescence
2. Leaching of active phases and supports
3. Poisoning of strongly adsorbed molecules

Because the cost of these noble metal catalysts used in theses reactions are very high, this problem must be concerned.

Silica (SiO_2) is one of the most useful supports. Although it is a naturally occurring material in minerals, most of the silica used in catalyst applications is amorphous silica of synthetic origin. Surface area, pore volume, pore size and particle size are to some extent independently controllable by the preparation conditions.

Sol-gel preparation is widely used in glass and ceramic industries as well as in catalyst preparation. Sols are dispersions of colloidal particles (size 1 - 100 nm) in a liquid. A gel is an interconnected, rigid network with pores of submicrometer dimensions and polymeric chains whose average length is greater than a micron. Sol-gel-derived silica has been prepared for the few decades; it offers a number of advantages such as mild process condition, high purity, and large surface area due to its nanosize.

1.2 Objective

The objective of this research is to investigate the characteristics and catalytic properties of sol-gel-derived silica supported Pd catalysts in liquid-phase hydrogenation reaction.

1.3 Scopes of work

1. Preparation of silica by sol-gel method with various particle sizes.
2. Preparation of silica-supported palladium catalyst (Pd/SiO_2) with 0.5-2% palladium loadings using ion-exchange and incipient wetness impregnation method
3. Characterization of silica-supported palladium catalysts using several techniques such as atomic absorption spectroscopy (AAS), X-ray diffraction (XRD), scanning electron microscopy (SEM), transmission electron microscopy (TEM), N_2 physisorption, X-ray photoelectron spectroscopy (XPS) and pulse CO chemisorption
4. Reaction study of silica-supported palladium catalysts in liquid phase hydrogenation of an alkene or alkyne using stirring batch reactor (stainless steel autoclave 50 ml)
5. Study of catalyst deactivation after performing liquid-phase hydrogenation.

CHAPTER II

THEORY

2.1 Sol-Gel (Hydrolysis and Condensation of Silicon Alkoxides)

Silicate gels are most often synthesized by hydrolyzing monomeric, tetrafunctional alkoxide precursors employing a mineral acid (e.g., HCl) or base (e.g., NH_3) as a catalyst. At the functional group level, three reactions are generally used to describe the sol-gel process:

<div align="center">

hydrolysis

$\equiv Si - OR + H_2O \quad \longleftrightarrow \quad \equiv Si - OH + ROH$

esterification

alcohol condensation

$\equiv Si - OR + HO - Si \equiv \quad \longleftrightarrow \quad \equiv Si - O - Si \equiv + ROH$

alcoholysis

water condensation

$\equiv Si - OH + HO - Si \equiv \quad \longleftrightarrow \quad \equiv Si - O - Si \equiv + H_2O$

hydrolysis

</div>
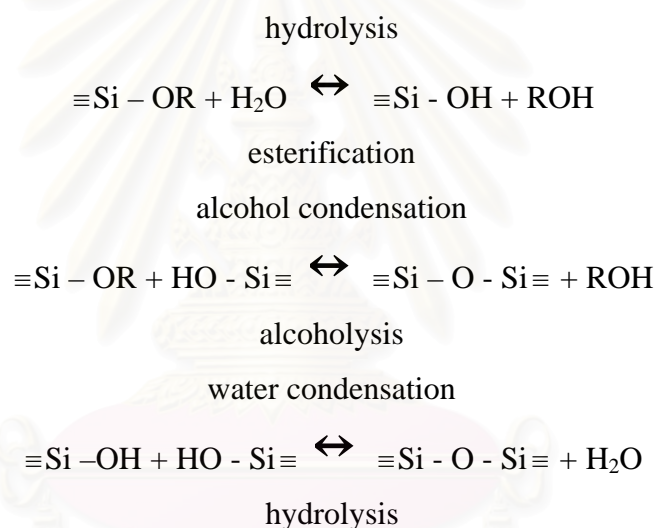
where R is an alkyl group, C_xH_{2x+1}. The hydrolysis reaction replaces alkoxide groups (OR) with hydroxyl groups (OH). Subsequent condensation reaction involving the silanol groups produce siloxane bonds (Si-O-Si) plus the by product alcohol (ROH) or water. Under most conditions, condensation commences before hydrolysis is complete. Because water and alkoxysilanes are immiscible, a mutual solvent such as alcohol is normally used as homogenizing agent. However, gels can be prepared from silicon alkoxide-water mixtures without added solvent, since alcohol produced as the by-product of hydrolysis reaction is sufficient to homogenize the initially phase separated system. It should be noted that alcohol is not simply a solvent.

2.2 Hydrogenation Reaction

One of the oldest and most diverse catalytic processes is the selective hydrogenation of functional groups contained in organic molecules to produce (i) fine chemicals (ii) intermediates used in pharmaceutical industry (iii) monomers for production of various polymers and (iv) fats and oils for producing edible and nonedible products. Indeed there are more hydrogenation catalysts available commercially than any other type, and for good reason, because hydrogenation is one of the most useful, versatile and environmentally acceptable reaction routes for organic synthesis. Hydrogenation processes are often made on a small scale in batch reactor. Batch processes are usually most cost effective since the equipment need not to be dedicated to a single reaction. Generally, large stirred autoclave is capable of H_2 pressure up to140 atm. Typically the catalyst is powdered and slurried with reactant; a solvent is usually present to influence product selectivity and to adsorb the reaction heat liberated by the reaction. Since most hydrogenations are highly exothermic, careful temperature control is required to achieve the desired selectivity and to prevent temperature runaway.

Addition of hydrogen to a carbon-carbon double bond is called hydrogenation. The overall effect of such an addition is the reductive removal of the double bond functional group. Regioselectivity is not an issue, since the same group (a hydrogen atom) is bonded to each of the double bond carbons. The simplest source of two hydrogen atoms is molecular hydrogen (H_2), but mixing alkenes with hydrogen does not result in any discernable reaction. Although the overall hydrogenation reaction is exothermic, a high activation energy prevents it from taking place under normal conditions. This restriction may be circumvented by the use of a catalyst, as shown in the following diagram.
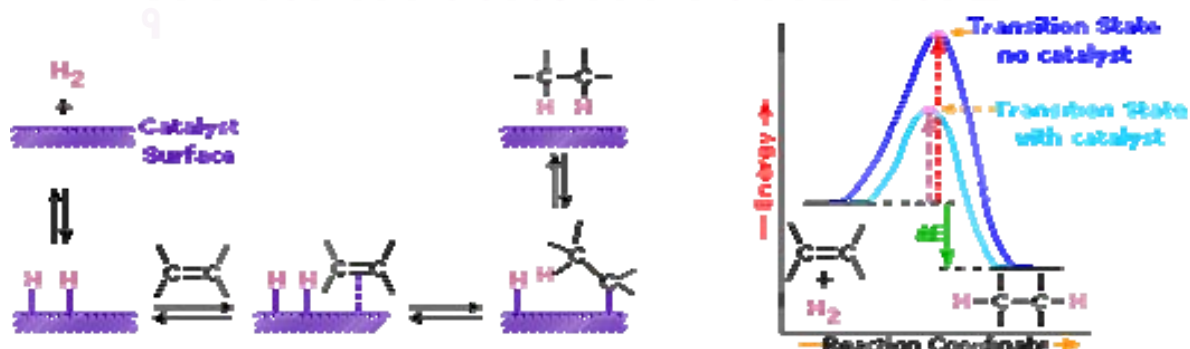
Catalysts are substances that change the rate (velocity) of a chemical reaction without being consumed or appearing as part of the product. Catalysts act by lowering the activation energy of reactions, but they do not change the relative potential energy of the reactants and products. Finely divided metals, such as platinum, palladium and nickel, are among the most widely used hydrogenation catalysts.

As shown in the energy diagram, the hydrogenation of alkenes is exothermic, and heat is released corresponding to the ΔE in the diagram. This heat of reaction can be used to evaluate the thermodynamic stability of alkenes having different numbers of alkyl substituents on the double bond.

Phenylacetylene hydrogenation scheme consists of two consecutive steps in parallel with a single step directly to the final hydrogenation product.
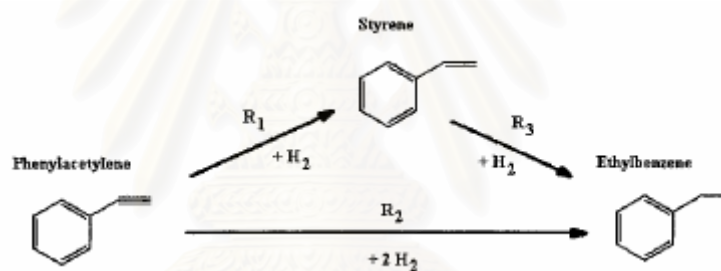
Cyclohexene hydrogenation scheme

2.3 Hydrogenation Catalyst

The types of hydrogenation catalysts found in commercial applications include noble metals, group VIII transition metals, organometallic complexes and activated alloy catalysts that are either unsupported or supported. The major advantages of noble metal catalysts are their relatively high activity, mild process conditions, easy separation and better handling properties. The most commonly used noble metals are

Pt, Pd, Rh and Ru. Generally Pd is more active than Rh or Pt for many hydrogenation reactions on the same carbon carrier. In general, using of support allows the active component to have a larger surface area, which is particularly important in those cases where a high temperature is required to activate the active component. The supports may be as different as carbon, silica, alumina and polymer in order to obtain higher selectivity and activity. Supported catalyst may be prepared by a variety of methods, depending on the nature of active components as well as the characteristics of carriers such as decomposition, precipitation, coprecipitation, adsorption and ion-exchange etc.

CHAPTER III

LITERATURE REVIEWS

3.1 Supported Pd catalyst in liquid-phase hydrogenation

Joice *et al.* (1994) studied palladium catalysts using X-ray photoelectron spectroscopy (XPS). Several palladium chloride and palladium acetate, complexes of polymer coated silica were used as recyclable hydrogenation catalysts. Hydrogenation studies were performed under an ambient pressure of H_2, in methanol solvent at room temperature. These catalysts had excellent activity over cycles of hydrogenation without any significant loss of metal or activity. The oxidation states of Pd and N were studied using XPS technique. It was indicated that the more active form of catalyst is the one, which contained Pd(O) or a mixture of Pd(II) and Pd(O).

Palinko (1995) studied effects of surface modifiers on the liquid-phase hydrogenation of alkenes over silica-supported platinum, palladium and rhodium catalysts in the presence of quinoline or carbon tetrachloride at room temperature. The catalysts were prepared with impregnation or ion-exchange methods. The result showed that the rate of hydrogenation decreases over Pd/SiO_2 and Rh/SiO_2 with increasing the amount of surface modifiers. Furthermore quinoline effectively deactivates the palladium and rhodium catalysts in cyclohexene hydrogenation, but residual activity for 1-hexene hydrogenation is above 50% for each of the catalysts used.

Jackson and Shaw (1996) studied the hydrogenation of cyclopentene, cyclohexene, cycloheptene and cis-cyclooctene over Pd/alumina, Pd/carbon, Pd/silica and Pd/zirconia catalysts. The hydrogenation reaction and the carbon deposition reaction showed evidence for particle size sensitivity and the trend in activity with particle size was not the same for all the cycloalkenes, with cycloheptene hydrogenation increasing with particle size. This behavior can principally be related to the strength and mode of adsorption of the cycloalkene, although the adsorbed state of hydrogenation may also influence reactivity.

Arunajatesan *et al.* (2001) studied fixed-bed hydrogenation of organic compounds in supercritical carbon dioxide. Pd/C was used as the catalyst in hydrogenation of cyclohexene to cyclohexane. The reaction was performed at near critical temperature of 343 K and at pressure of 13.6 MPa. The excellent temperature control and stable catalyst activity were observed. It indicates that the near critical reaction medium has sufficient heat capacity to effectively remove the heat of reaction.

Nozoe *et al.* (2001) studied the non-solvent hydrogenation of solid alkynes and alkenes using supported palladium catalysts. Trans-stibene and carboxylic acid with α,β C=C bonds were employed as the alkene-type substrates for the non-solvent hydrogenation. Their hydrogenation proceeded over Pd/SiO_2 catalyst at room temperature. The hydrogenation rate of trans-stibene under the non-solvent condition was lower than the hydrogenation in tetrahydrofuran (THF).

Singh and Vannice (2001) studied liquid-phase citral hydrogenation over SiO_2-supported group VIII metals. The reaction was carried out in glass reactor at 300 K and atmospheric pressure. The initial TOF for citral hydrogenation exhibited the following trend: Pd > Pt> Ir> Os > Ru > Rh > Ni > Co >> Fe. With the exception of Ni/SiO_2, all catalysts exhibited substantial deactivation due to citral and/or unsaturated alcohol decomposition to yield adsorbed CO that poisoned active sites responsible for hydrogenation. In contrast, Ni/SiO_2 exhibited an initially low TOF that increased fourfold after 7 h of reactions after which time no deactivation was detected up to 84% conversion.

Tschan *et al.* (2001) studied Continuous Semihydrogenation of Phenylacetylene over Amorphous $Pd_{81}Si_{19}$ Alloy in "Supercritical" Carbon Dioxide. It was found that high conversion and selectivity were achieved over this catalyst without chemical modification, usually applied for Lindlar-type catalysts. Hydrogenation of PA to ST yielded the highest conversions and good selectivities at the edge of the sc single-phase region. Moreover, excess hydrogen in the system leads to overhydrogenation of PA and thus to a steady decrease in selectivity.

Juszczyk *et al.* (2002) studied transformation of Pd/SiO$_2$ catalysts during high temperature reduction. It was shown that the considerable interactions between palladium and silica occurred even reduction in dihydrogen at low temperature and the silica-supported palladium catalyst was converted to Pd$_4$Si. The reaction of 2,2-dimethylpropane with dihydrogen was used to studied the catalytic properties of Pd$_4$Si. It was revealed that the catalytic activity and the activation energy decreased while the selectivity toward isomerization (at expense of hydrogenolysis) increased.

Pillai *et al.* (2002) studied maleic anhydride hydrogenation over Pd/Al$_2$O$_3$ catalyst under supercritical CO$_2$ medium. The catalyst was prepared by wet impregnation of alumina pellets with palladium chloride solution. The experiments were carried out in stainless steel batch reactor and the reactions were studied at different temperature and pressure. The result showed that temperature is critical in obtaining the desired high γ-butyrolactone selectivity. However increasing the hydrogen partial pressure or temperature is found to favor the lactone formation. Furthermore, the selective hydrogenation of a low vapor pressure compound like maleic anhydride can be successfully carried out in supercritical CO2 medium.

Tanaka *et al*. (2002) prepared Pd/SiO$_2$ catalysts by a complexing agent assisted sol-gel method and impregnation method using and organic complexing agent or water as the impregnation solvent. The Pd/SiO$_2$ were characterized by TG-DTA, FT-IRs, C-NMR, XRD, TM XPS and CO adsorption. The difference between the preparation method was discussed. The result showed that the palladium particles in the sol-gel catalysts were much smaller and more uniform in size than those in the corresponding impregnation catalysts.

Dominguez-Quintero *et al.* (2003) investigated palladium nanoparticle in hydrogenation catalysis of different substrate (1-hexene, cyclohexene, benzene, 2-hexanone and benzonitrile).Palladium nanoparticles (1.9 nm) stabilized was obtained from the reduction of organometallic precursor (palladium(II)bis-dibencylidene acetone) with hydrogen. The highest hydrogenation rate was found with 1-hexene with TOF of 38250 mole of product/mole of metal/h at 25°C and 30 psi pressure. They presented that the catalytic potential of the Pd/SiO$_2$ synthesized by

organometallic route renders an extremely active nanomaterial which shows little aggregation after catalytic reaction even 145°C.

Min *et al*. (2003) studied silica-supported metal catalysts using Pd/silica as a case study since noble metals supported on SiO_2 have attracted considerable attention due to the importance of the silica-metal interface in heterogeneous catalysis and in electronic device fabrication. It was shown that metals supported on SiO2 exhibited a metal-support interaction that varied from weak to strong, depending upon the metal, after high temperature treatments. A strong metal-support interaction, manifested as encapsulation, inter-diffusion, and alloying can alter the catalytic properties significantly. More importantly, it was shown that defects, e.g. oxygen vacancies or excess Si, play a critical role in determining the strength of the metal-support interaction.

Pillai *et al.* (2003) studied hydrogenation of 4-Oxoisophorone over a Pd/Al_2O_3 catalyst under supercritical CO_2 medium at different reaction conditions. The catalyst was prepared by wet impregnation of alumina pellets with 0.1 M palladium chloride. Isothermal hydrogenation was conducted in a 500 ml stainless steel batch reactor. Phase behavior studies showed that 4-Oxoisophorone forms a supercritical phase with a H_2-CO_2 mixture at 373 K and at a total pressure of 15 MPa with a H_2 partial pressure of 1.7 MPa. The result revealed that CO_2-organic cosolvent systems do not show any advantage at the conditions employed. The extent of deactivation is much lower for the reaction in supercritical CO_2 than in organic solvent.

Yamada and Goto (2003) studied the effect of solvents polarity on selective hydrogenation of unsaturated aldehyde in gas-liquid-solid three phase reactor. Pd/C, Pt/C and Co/Al_2O_3 were used as the catalysts. Experiments were carried out in a semi-batch stirred tank reactor. Hydrogen gas was introduced continuously in the reactor. The solvents were various normal alcohols and various aromatic compounds. They found that polar solvents activate a polar double bond C=O and non-polar solvents activate a non-polar double bond C=C.

Burgener *et al.* (2004) studied hydrogenation of citral over Pd/alumina by comparison of supercritical CO_2 and conventional solvents in continuous and batch reactor. The experiment revealed that citral hydrogenation is remarkably faster in single-phase reaction mixture using supercritical carbon dioxide than using organic solvents (hexane and dioxane). As the activity of Pd/alumina was mainly limited to the saturation of C=C bonds of citral in all three solvents, this comparison is not distorted by the different nature of reactions.

Panpranot *et al.* (2004) studied the impact of the silica support structure on liquid-phase hydrogenation on Pd catalysts. SiO_2 (d_{pore} = 3 nm), SiO_2 (large pore), MCM-41 (d_{pore} = 3 nm) and MCM-41 (d_{pore} = 9 nm), referred as S-3nm, S-large, M-3nm and M-9nm respectively, were used as supports. The catalysts were prepared by incipient wetness impregnation. The reaction was carried out at $25^{o}C$ and 1 atm in a stainless steel Parr autoclave. The results showed that for the larger pore supports (S-large and M-9nm), Pd particles likely formed primarily in the pores, whereas use of smaller pore supports resulted in Pd particles primarily on the outside surface of the catalyst granules (S-3nm) or both inside and outside the support pores (M-3nm). All the catalysts exhibited similar TOFs for the liquid-phase hydrogenation of 1-hexene. The Pd particle size appeared to strongly determine this metal loss during reaction. However, it is also likely that the location on the silica support also played an important role.

Panpranot *et al.* (2004) studied the differences between Pd/SiO_2 and Pd/MCM-41 catalysts in liquid-phase hydrogenation. SiO_2-small pore, SiO_2-large pore, MCM-41-small pore and MCM-41-large pore were used as supports. The catalysts were prepared by incipient wetness impregnation. The reaction was carried out at $25^{o}C$ and 1 atm in a stainless steel Parr autoclave. The results showed that the characteristics and catalytic properties of the silica supported Pd catalysts in liquid-phase hydrogenation were affected by type of silica, pore size and pore structure. The catalyst activities were found to be merely dependent on the Pd dispersion, which as itself a function of the support pore structure. Among the four types of the supported Pd catalysts used in this study, Pd/MCM-41-large pore showed the highest Pd dispersion and the highest hydrogenation rate with the lowest amount of metal loss.

3.2 Deactivation of supported Pd catalysts in liquid-phase reaction

Albers *et al.* (2001) studied the major causes for deactivation such as particle growth, coke deposition and leaching. They found that the leaching of precious metal can be minimized by either improving the availability of hydrogen in the liquid reaction medium or by optimizing the catalyst side of the process. In term of modifying the catalyst site of the process two approaches are proposed (i) Using of smaller quantities of catalyst for reaction and/or (ii) decreasing the precious metal loading of catalyst. Unfavorable and undesired effect about sintering and agglomeration may be suppressed by means of adequate impregnation agents and procedures, temperature control and using suitable support materials.

Besson and Gallezot (2003) reviewed the factors contributing to the deactivation of metal catalysts employed in liquid-phase reaction for the synthesis of fine or intermediate chemicals. The main causes of catalyst deactivation are particle sintering, metal and support leaching, deposition of inactive metal layers or polymeric species and poisoning by strongly adsorbed species. Leaching of metal atoms depends upon the reaction medium (pH, oxidation potential, chelating properties of molecules) and upon bulk and surface metal properties.

Heidenreich *et al*. (2002) studied the parameter that influence the palladium leaching during and after Heck reactions of aryl bromides with olefins catalyzed by heterogeneous Pd on activated carbon systems. The results showed that the Pd concentration in solution correlated with the nature of the starting materials and products, the temperature, the solvent, the base and the atmosphere (argon and air). Lower temperature, higher concentration and stronger interaction of the bromoarenes with Pd^0 clearly increase Pd leaching.

3.3 Comment on the previous works

From literature reviews, Pd is the one of the most useful catalysts used in liquid-phase hydrogenation reaction. Furthermore types of solvent and support show the important roles in catalytic activity and catalyst deactivation. In the recent years, supercritical carbon dioxide has been increasingly used as an environmentally friendly

reaction medium in place of toxic and hazardous organic solvents. However catalyst deactivation such as leaching is the problem that usually occurs in these reactions. Sol-gel-derived silica has shown to offer a number of advantages such as mild process condition, high purity, and large surface area due to its nanosize, however, the properties of Pd catalysts supported sol-gel-derived silica in catalytic liquid-phase hydrogenation and deactivation have not been well studied so far. Thus it is the aim of this study to synthesize nano-silica by sol-gel technique and apply as Pd catalyst support in liquid-phase hydrogenation.

CHAPTER IV

EXPERIMENTAL

4.1 Catalyst Preparation

Catalyst supports used in this study are sol gel-derived silica and silica-large pore (commercial silica) from Strem Chemicals and are denoted as silica-SG and silica-com, respectively.

4.1.1 Synthesis of Silica

Sol gel-derived silica used in this experiment is synthesized by sol-gel method. The compositions of gel are 40 ml of tetraethylorthosilicate (TEOS), 10.5 ml of ethanol, 12.5 ml of water and 1 ml of hydrochloric acid (HCl). The mixtures are vigorously stirred for 1 hr. Then the gel is calcined for 6 h at 500°C

Table 4.1 Chemicals used in the synthesis of silica

Chemical	Supplier
Tetraethylorthosilicate (TEOS)	Aldrich
Absolute ethyl alcohol (99.99vol. %)	Aldrich
Hydrochloric acid (30%)	Carlo Erba

4.1.2 Palladium Loading

In this experiment, ion-exchange and incipient wetness impregnation are the two methods used for loading palladium. $Pd(NH_3)_4Cl_2$ is used as precursor in both methods.

The ion-exchange procedure is as follow :
1. The certain amount of palladium (1% loading) and 1 g of silica are introduced into 40 ml of water.

2. The pH of mixture is adjusted to 12 by using 25% NH_4OH.

3. Then the mixture is vigorously stirred for 3 days.

4. The residue solid is filtrated and washed with distilled water until the pH is reduced to 7.

5. The catalyst is dried in the oven at 100^oC overnight.

6. Then the catalyst is calcined in air at 450^oC for 3 h

The incipient wetness impregnation procedure is as follow :

1. The certain amount of palladium (1% loading) is introduced into the water which its volume equals to pore volume of catalyst.

2. Silica support is impregnated with aqueous solution of palladium. The palladium solution is dropped slowly to the silica support.

3. The catalyst is dried in the oven at 100^oC overnight.

4. The catalyst is calcined in air at 450^oC for 3 h

Table 4.2 Chemicals used for palladium loading

Palladium precursor	Supplier
Tetraamminepalladium(II)chloride ($Pd(NH_3)_4Cl_2$)	Aldrich
Aqueous solution of 25% NH_3	Merck

4.2 The Reaction Study in Liquid-Phase Hydrogenation

The liquid-phase hydrogenation is used to study the characteristic and catalytic properties of these prepared catalysts. An alkene and aromatic such as cyclohexene and phenylacetylene are used as reactants. Supercritical carbon dioxide and several organic solvents are used as reaction medium.

4.2.1 Chemicals and Reagents

The chemicals and reagents used in the reactions are shown in Table 4.3

Table 4.3 The chemicals and reagents used in the reaction

The chemicals and reagents	Supplier
High purity grade Hydrogen (99.99vol. %)	Thai Industrial Gases Limited
Carbon dioxide	Mallinckrodt
Absolute ethyl alcohol (99.99vol. %)	Aldrich
Benzene	Panreac Quimica
Cyclohexene (96vol. %)	Merck
Heptanol	Merck
Normal methyl pyrrolidone	Fluka
Phenylacetylene	Aldrich

4.2.2 Instruments and Apparatus

The schematic diagram of liquid-phase hydrogenation is shown in Figure 4.1. The main instruments and apparatus are explained as follow:

The autoclave reactor

The 50 ml stainless steel autoclave was used as reactor. Hot plate stirrer with magnetic bar was used to heat up the reactant and to ensure that the reactant and the catalyst are well mixed.

Supercritical carbon dioxide pump

The PU-1580-CO_2 is a liquid CO_2 delivery system using SSQD (Slow Suction Quick Delivery) method. The maximum usable pressure is 30 MPa. The operating temperature range is between 10 to 30°c.

Gas chromatography

A gas chromatography equipped with flame ionization detector (FID) with GS-alumina capillary column was used to analyze the feed and product

Table 4.4 Operating conditions for the gas chromatograph

Gas Chromatograph	Shimadzu GC-14A
Detector	FID
Packed column	GS-alumina (length =30 m, I.D. = 0.53 mm)
Carrier gas	Helium (99.99vol. %)
Make-up Gas	Nitrogen (99.99vol. %)
Flow rate of carrier gas	25 cc/min
Flow rate of make-up gas	45
Column temperature	200°C
Detector temperature	250°C
Injector temperature	280°C

4.2.3 Liquid-Phase Hydrogenation Procedure

The reaction study section is divided into two parts. The first part is phenylacetylene hydrogenation which performed in ethanol solvent and the second part is cyclohexene hydrogenation which carried out in conventional organics solvents (such as benzene, heptanol, and normal-methyl pyrrolidone), under high pressure CO_2 and under solvent less.

4.2.2.1 Phenyl acetylene hydrogenation procedures are consisted of 2 steps.
1. Reduction step

Approximately 0.1 gram of supported Pd catalyst was placed into the quartz tube. Then the catalyst was reduced by the hydrogen gas at the volumetric flow rate of 50 ml/min at room temperature for 2 h.

2. Reactant preparation and hydrogenation step

1 ml of phenyl acetylene, 9 ml of ethanol and 0.1 gram of catalyst were introduced into the autoclave reactor. Afterward the reactor was filled with hydrogen at 1 bar pressure. The liquid phase hydrogenation was carried out at room temperature for 1 h. After the reaction the vent valve was slowly opened to prevent the loss of

product. Then the product mixture was analyzed by gas chromatography with flame ionization detector (FID) and the catalyst was characterized by several techniques.

4.2.2.2 Cyclohexene hydrogenation procedures are also consisted of 2 steps.

1. Reduction step

This procedure was the same as the reduction step in phenylacetylene hydrogenation.

2. Reaction step

1 ml of cyclohexene, 24 ml of conventional organic solvents such as benzene, heptanol and normal methyl pyrrolidone denoted as NMP and 0.1 gram of catalyst were introduced into the autoclave reactor. Afterward the reactor was filled with hydrogen to 10 bar. For the case of using supercritical carbon dioxide as medium the reactant and the catalyst were introduced into the autoclave reactor without any organic solvent. The supercritical carbon dioxide was pumped to the reactor by supercritical carbon dioxide pump to the desired pressure. The reaction was performed at room temperature for 10 minutes. After the reaction the vent valve was slowly opened to prevent the loss of product. Then the product mixture was analyzed by gas chromatography with flame ionization detector (FID) and the catalyst was characterized by several techniques.

4.3 Catalyst Characterization

The fresh and spent catalysts were characterized by several techniques such as

4.3.1   Atomic Absorption Spectroscopy (AAS)

The bulk composition of palladium was determined using a Varian Spectra A800 atomic adsorption spectrometer at the Department of science service Ministry of science technology and environment.

4.3.2 N₂ Physisorption

The surface area of solid, pore volumes, average pore size diameters and pore size distribution were determined by physisorption of nitrogen (N_2) using Micromeritics ASAP 2020 (surface area and porosity analyzer)

4.3.3 X-ray Diffraction (XRD)

The bulk crystal structure and chemical phase composition were determined by diffraction of an X-ray beam as a function of the angle of the incident beam. The XRD spectrum of the catalyst is measured by using a SIEMENS D500 X-ray diffractometer and Cu K_α radiation. The crystallite size was calculated from Scherrer's equation.

4.3.4 Scanning Electron Microscopy (SEM)

Catalyst granule morphology was obtained using a JEOL JSM-35CF scanning electron microscope operated at 20 kV at the Scientific and Technological Research Equipment Center, Chulalongkorn University (STREC).

4.3.5 Transmission Electron Microscopy (TEM) with the diffraction mode

Catalyst crystallite sizes and the diffraction pattern of silica supports were obtained using the JEOL JEM 2010 which employs a LaB6 electron gun in the voltage range of 80 to 200 kV with an optical point to point resolution of 0.23 nm at National Metal and Materials Technology Center.

4.3.6 CO-Pulse Chemisorption

The active sites and the relative percentages dispersion of palladium catalyst were determined by CO-pulse chemisorption technique using Micromeritics ChemiSorb 2750 (pulse chemisorption system)

4.3.7   X-ray Photoelectron Spectroscopy XPS

The XPS spectra, the binding energy and the composition on the surface layer of the catalysts were determined by using a Kratos Amicus X-ray photoelectron spectroscopy. The analyses were carried out with these following conditions: Mg Ka X-ray source at current of 20 mA and 12 kV, 0.1 eV/step of resolution, and pass energy 75 eV and the operating pressure was approximately 1×10^{-6} Pa
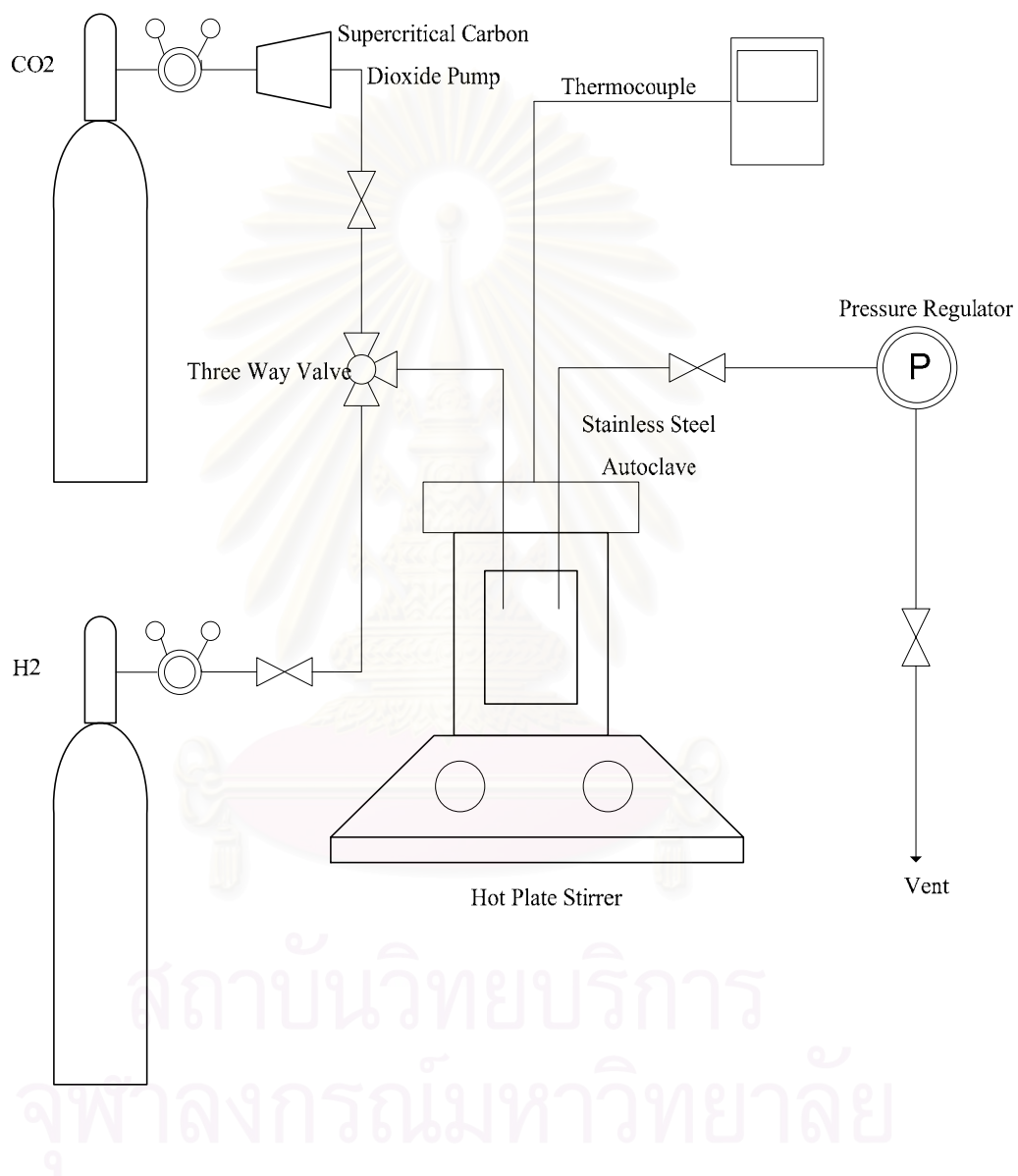
Figure 4.1 A schematic diagram of the liquid-phase hydrogenation system

CHAPTER V

RESULTS AND DISCUSSION

Supported noble metal catalysts are widely used in hydrogenation reactions. In this study the catalysts were prepared by two methods, impregnation and ion-exchange method. The results and discussions in this chapter are divided into two parts. In the first part the characteristics and catalytic properties of catalysts prepared by two different methods (Pd/SiO$_2$-SG-im, Pd/SiO$_2$-com-im, Pd/SiO$_2$-SG-ion and Pd/SiO$_2$-com-ion) were investigated in selective phenylacetylene hydrogenation. The reaction was carried out at 30°C and pressure 1 bar. The catalysts were characterized by several techniques such as SEM, TEM , N$_2$ physisorption, XRD, XPS, and CO-pulse chemisorption. The second part is cyclohexene hydrogenation using Pd/SiO$_2$ catalysts prepared by ion-exchange method. The reaction was performed at room temperature and 10 bar H$_2$ in different organic solvents, under pressurized carbon dioxide, and under solvent less condition. In this part the effects of solvents and carbon dioxide pressure on hydrogenation activity were studied. Furthermore, catalyst deactivations due to metal sintering and metal leaching were also investigated using AAS, XRD, and CO-chemisorption techniques.

5.1 Selective Hydrogenation of Phenylacetylene

5.1.1 Characterization of the Catalysts

5.1.1.1 Scanning Electron Microscopy (SEM)

Scanning electron microscopy (SEM) is a powerful tool for observing directly surface texture and morphology of catalyst materials. In the backscattering scanning mode, the electron beam focused on the sample is scanned by a set of deflection coils. Backscattered electrons or secondary electrons emitted from the sample are detected.

SEM micrographs of silica-SG and silica-com are shown in Figure 5.1(a) and 5.1(b), respectively. It was found that there were no differences in the appearance of both silica supports.
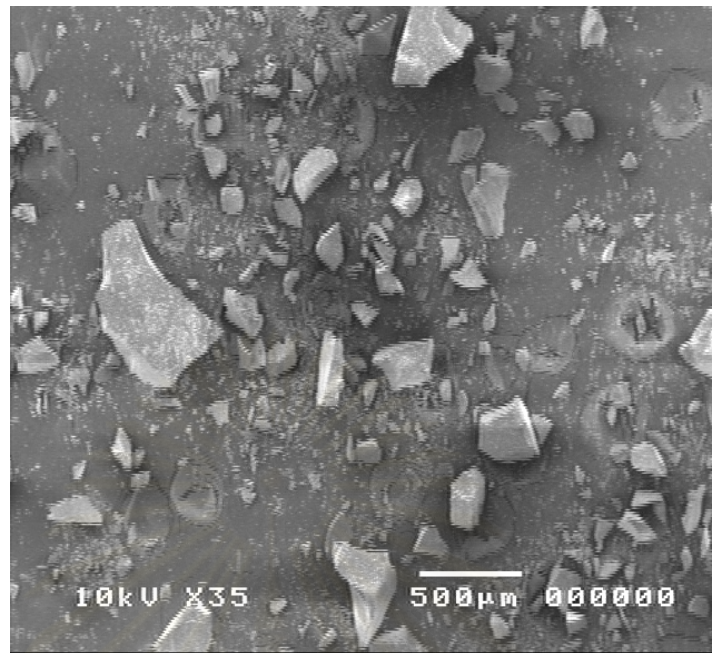
(a.)
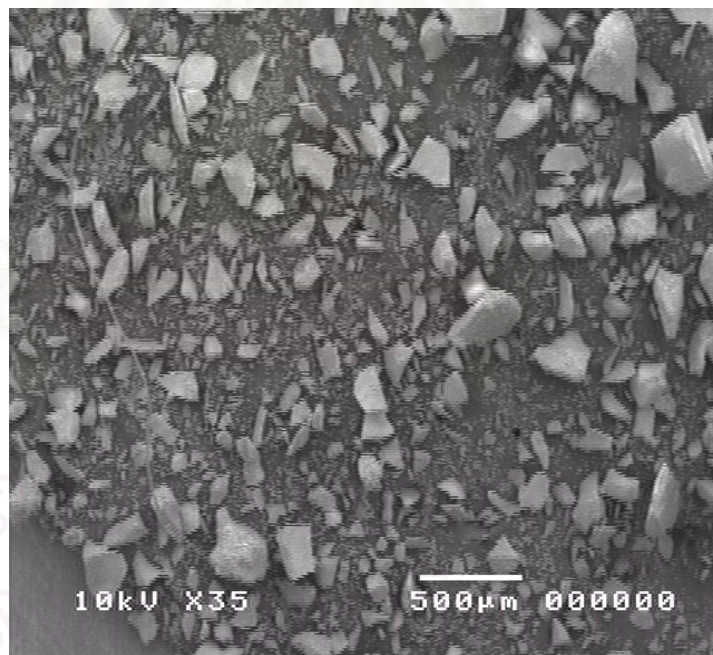
(b.)

Figure 5.1   SEM Micrographs of (a) SiO_2-SG (b) SiO_2-com

5.1.1.2 Transmission Electron Microscopy (TEM)

TEM micrographs were taken for silica-SG and silica-com in order to physically measure the size of supports. TEM with diffraction modes were used to determine the crystallographic structure of the supports. The TEM micrographs and the elemental diffraction results for silica-SG and silica-com are shown in Figure 5.2 and 5.3, respectively. According to Figure 5.2(a) and 5.3(a), it is revealed that the commercial silica is composed of many small particles with an average particle size of ca 17 nm. Compared to the commercial one, larger particle size was seen for the sol-gel derived silica. However, sol-gel method usually produces single crystalline oxides, the large particles observed maybe the secondary particles formed by agglomeration of the primary nano-particles due to heat treatment during calcinations step. From the elemental diffraction results, it is revealed that the silica-SG is semi-polycrystallite whereas the silica-com is absolutely amorphous.
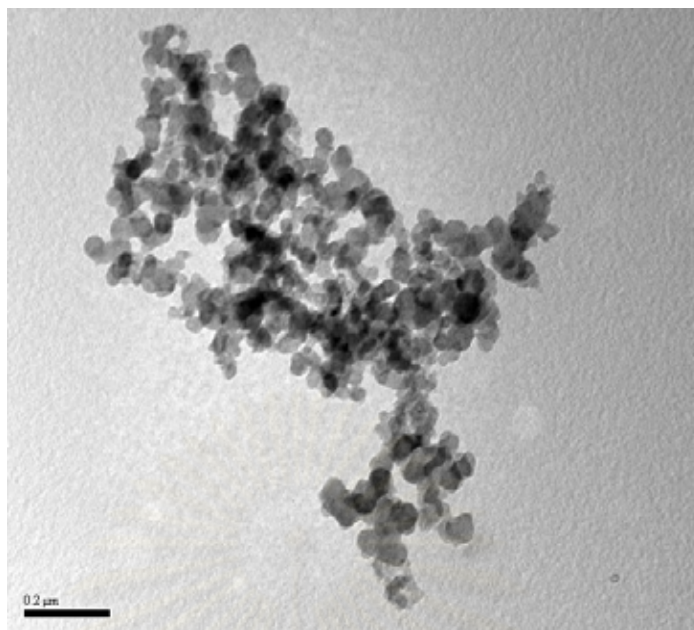
(a)

(b)

Figure 5.2 TEM micrographs of (a) SiO$_2$-SG (b) SiO$_2$-SG-diffraction mode
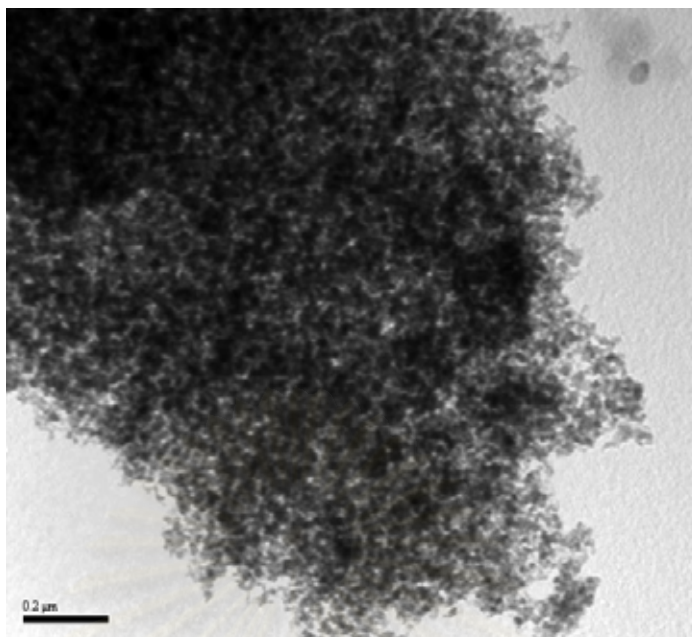
(a)
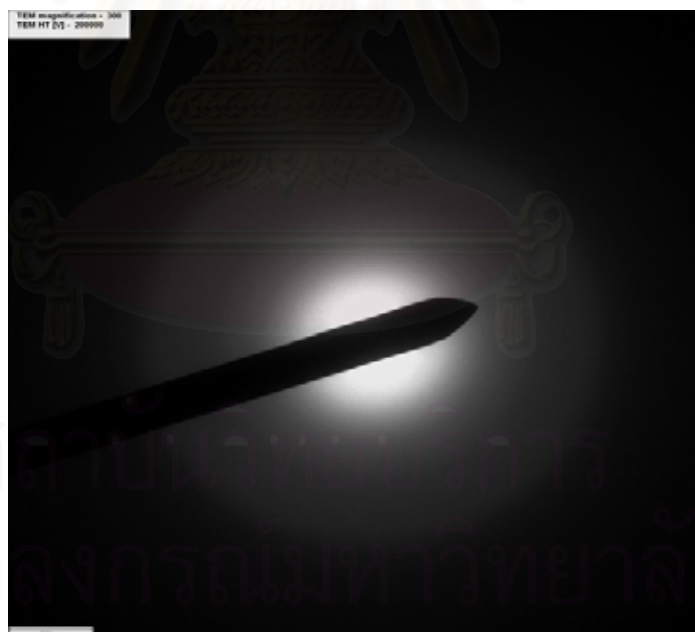
(b)

Figure 5.3 TEM micrographs of (a) SiO_2-com and (b) SiO_2-com-diffraction

5.1.1.3 N₂ Physisorption

BET surface areas, pore volumes and pore diameters of the silica and the silica-supported Pd were determined by N_2 physisorption technique and are shown in Table 5.1. The N_2 adsorption-desorption isotherms of the silica-SG and silica-com are shown in figure 5.5 and 5.6, respectively. It is indicated that the pores of silica-SG are micro pores whereas the pores of silica-com are macro pores. As shown in Table 5.1, BET surface areas of silica-SG and silica-com were 307.2 and 243.0 m^2/g, and pore volumes of silica-SG and silica-com were 0.145 and 1.060 cm^3/g, respectively. Because silica-SG had nano crystallite size, its BET surface areas are higher than that of silica-com.

After Pd loading by the impregnation method, BET surface areas of Pd-SG-im and Pd-com-im were 248.0 and 234.8 m^2/g, and pore volumes of Pd-SG-ion and Pd-com-ion were 0.118 and 1.017 cm^3/g, respectively. It can be seen that BET surface areas and pore volumes of the catalysts prepared by the impregnation method slightly decreased. Such results indicate that only a small amount of Pd was deposited in the pores of the silica. In contrast, the BET surface areas and pore volumes of the Pd/SiO₂ catalysts prepared by ion-exchange method dramatically decreased. BET surface areas of Pd-SG-ion and Pd-com-ion became 5.5 and 6.2 m^2/g and pore volumes of Pd-SG-ion and Pd-com-ion became 0.009 and 0.041 cm^3/g, respectively. It suggests that pore blockage or destruction of the silica pore structure occurred for these cases. Furthermore average pore diameters of both catalysts prepared by impregnation method did not change whereas average pore diameters for those prepared by ion-exchange method appreciably changed.

Table 5.1 N_2 physisorption properties of silica supports and Pd catalysts

Sample	N_2 physisorption		
	BET surface area (m^2/g)	Pore Volume (cm^3/g)	Avg Pore Diameter(nm)
silica-SG	307.2	0.145	1.89
silica-com	243.0	1.060	17.40
Pd/SiO$_2$-SG-im	248.0	0.118	1.91
Pd/SiO$_2$-com-im	234.8	1.017	17.32
Pd/SiO$_2$-SG-ion	6.2	0.009	5.93
Pd/SiO$_2$-com-ion	5.5	0.041	29.58
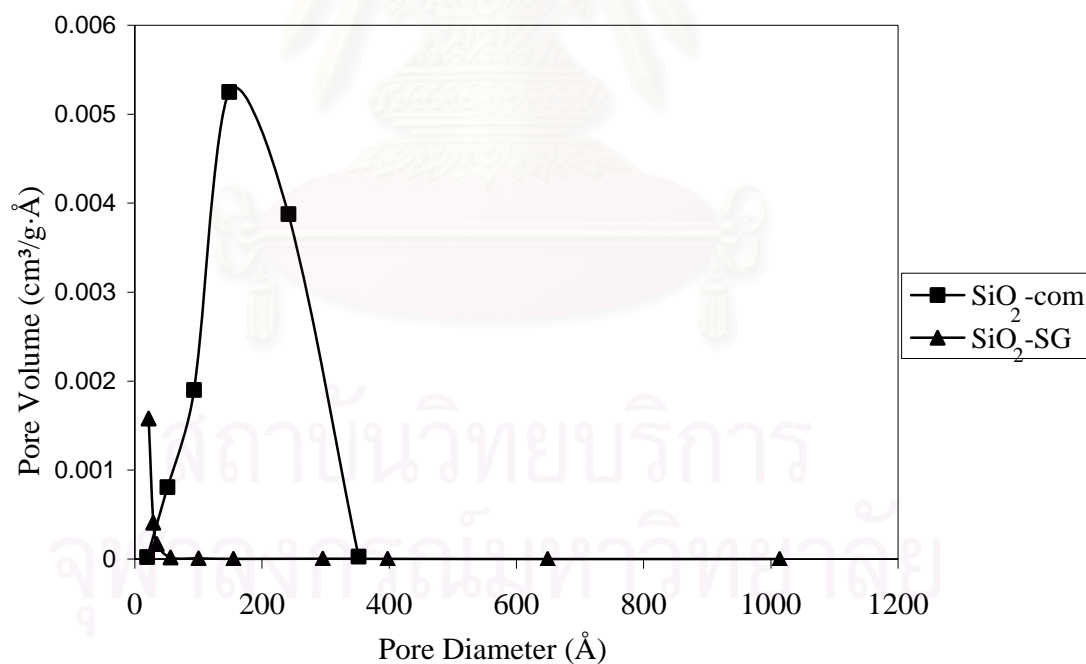
Figure 5.4 Pore size distributions of SiO$_2$-SG and SiO$_2$-com
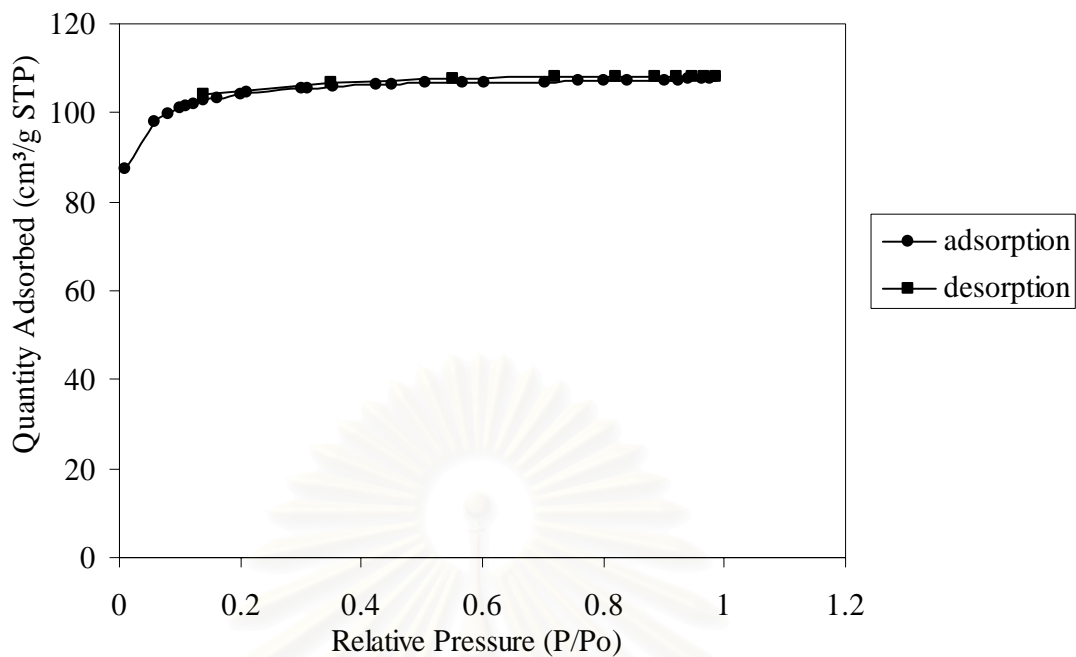
Figure 5.5 N$_2$ adsorption-desorption isotherms of SiO$_2$-SG
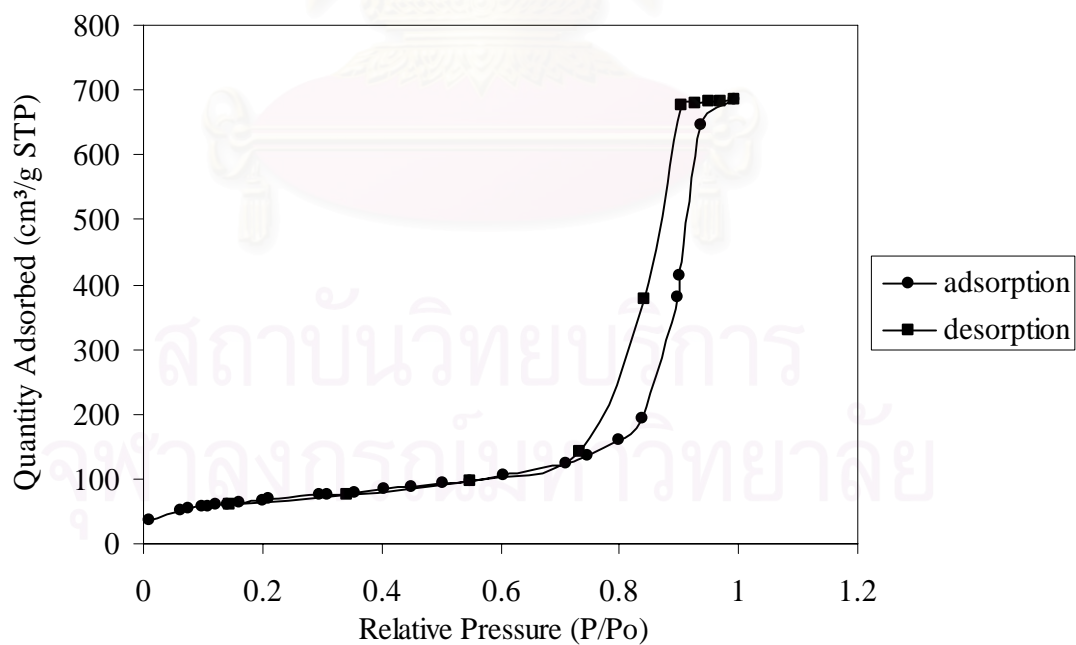
Figure 5.6 N$_2$ adsorption-desorption isotherms of SiO$_2$-com
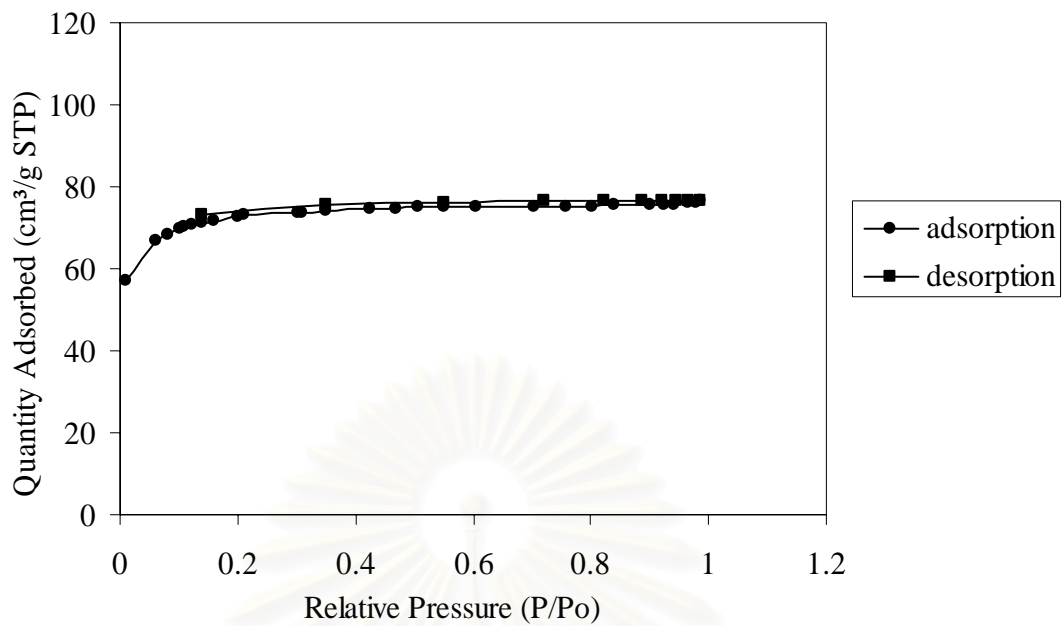
Figure 5.7 N$_2$ adsorption-desorption isotherms of Pd/SiO$_2$-SG-im
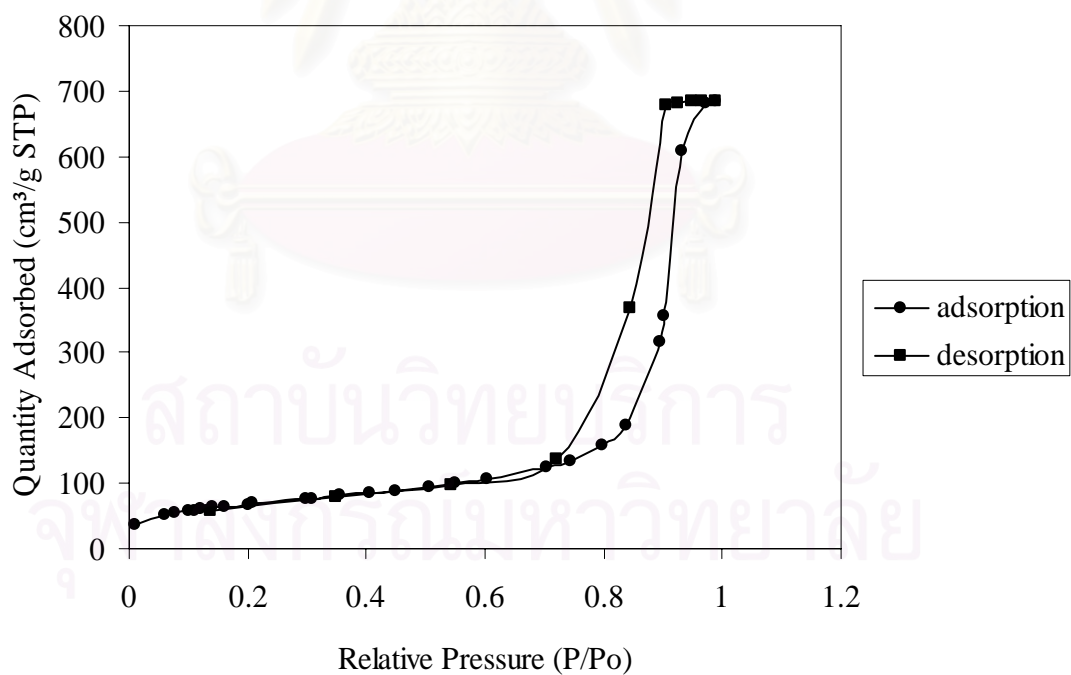
Figure 5.8 N$_2$ adsorption-desorption isotherms of Pd/SiO$_2$-com-im
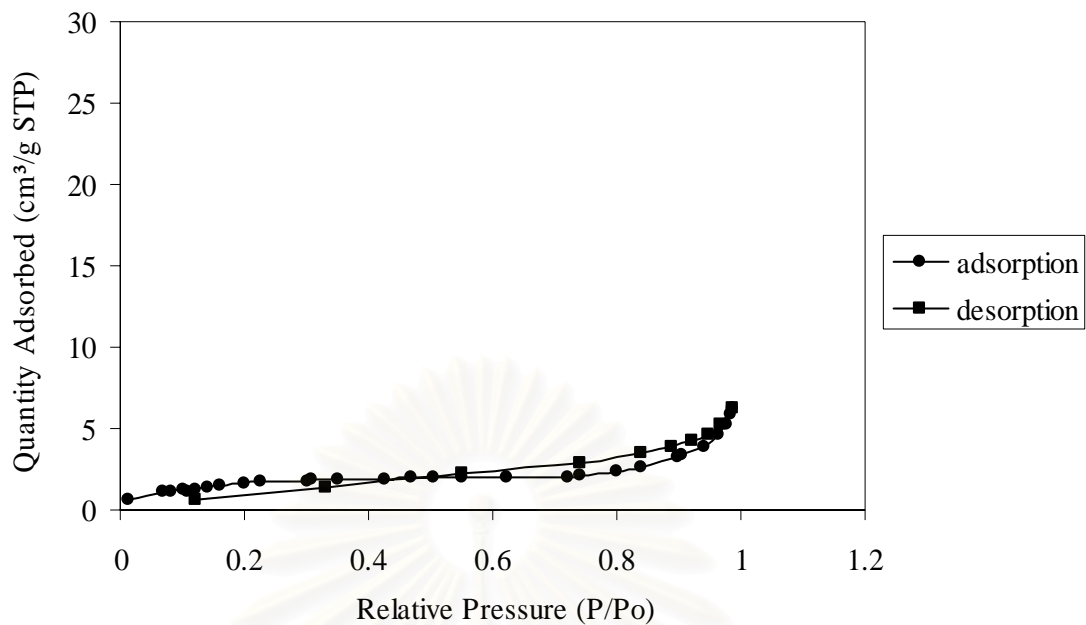
Figure 5.9 N_2 adsorption-desorption isotherms of Pd/SiO$_2$-SG-ion
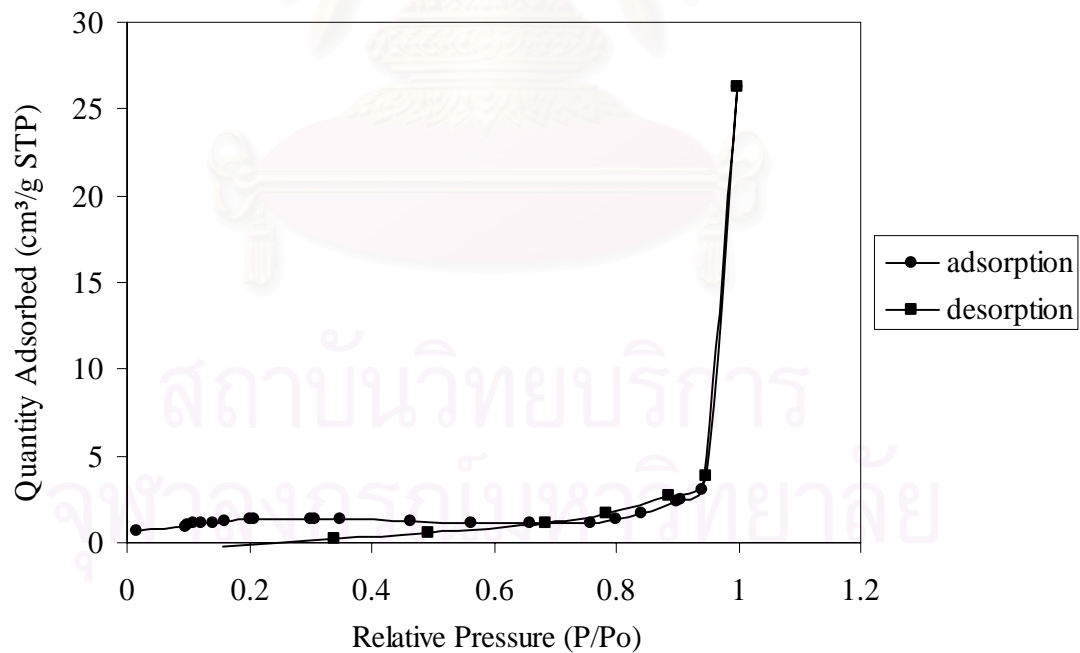
Figure 5.10 N_2 adsorption-desorption isotherms of Pd/SiO$_2$-com-ion

5.1.1.4 X-ray diffraction (XRD)

Bulk crystal structure and chemical phase composition of a crystalline material having crystal domains of greater than 3-5 nm can be detected by diffraction of an X-ray beam as a function of the angle of the incident beam. The measurements were carried out at the diffraction angles (2θ) between 10° and 80°. Broadening of the diffraction peaks were used to estimate crystallite diameter from Scherrer Equation.

The XRD patterns of silica-SG and silica-com support were carried out at the diffraction angles (2θ) between 10° and 80° are shown in Figure 5.11 There were no significant differences between these two support and only a broad peak was observed at $2\theta = 22^o$.

The XRD patterns of the various Pd/SiO_2 prepared by impregnation and ion-exchange method in the calcined state are shown in Figure 5.12 The XRD characteristic peaks for PdO at 2θ of ca. 33.8 and less so at 42.0, 54.8, 60.7, and 71.4^o were observed only for the catalysts prepared by impregnation method. The average PdO crystallite sizes on SiO_2-SG-im and SiO_2-com-im were calculated from the full width at half maximum of the XRD peak at 33.8^o 2θ using Scherrer's equation (Klug and Alexander) to be 9.6 and 11.3 nm, respectively and are shown in Table 5.2. For the catalysts prepared by ion-exchange method, it was found that palladium silicide was formed on the sol-gel derived silica as indicated by XRD characteristic peaks at $2\theta = 18.1^o$. The average palladium silicide crystallite size was calculated to be 61.2 nm as reported in Table 5.2. The XRD characteristic peaks of palladium silicide and/or PdO were not observed in the case of commercial silica supported Pd catalyst prepared by ion-exchange method, suggesting that Pd was probably highly dispersed and its average particle size was smaller than XRD detectable limit.

Table 5.2 Phases presented and crystallite sizes of fresh catalysts

Catalyst	XRD	
	phase	crystallite size (nm)
Pd-SG-im	PdO	9.6
Pd-com-im	PdO	11.34
Pd-SG-ion	PdSi	61.2
Pd-com-ion	n.d.*	n.d.

* n.d. = not determined.
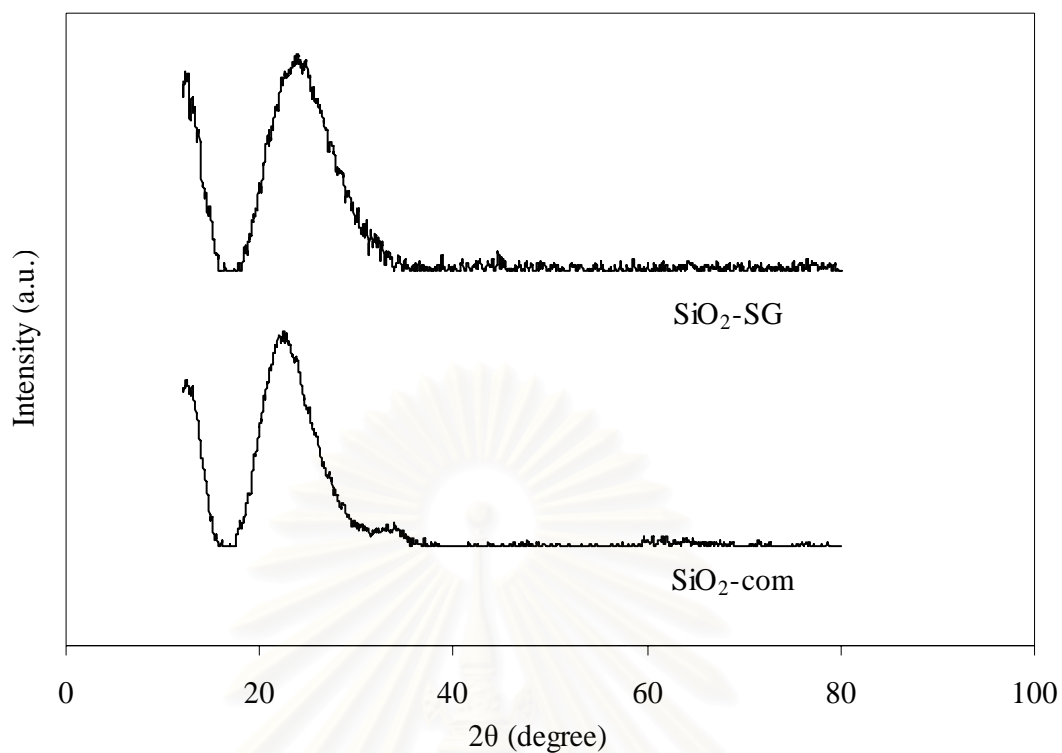
Figure 5.11 XRD patterns of SiO$_2$-SG and SiO$_2$-com
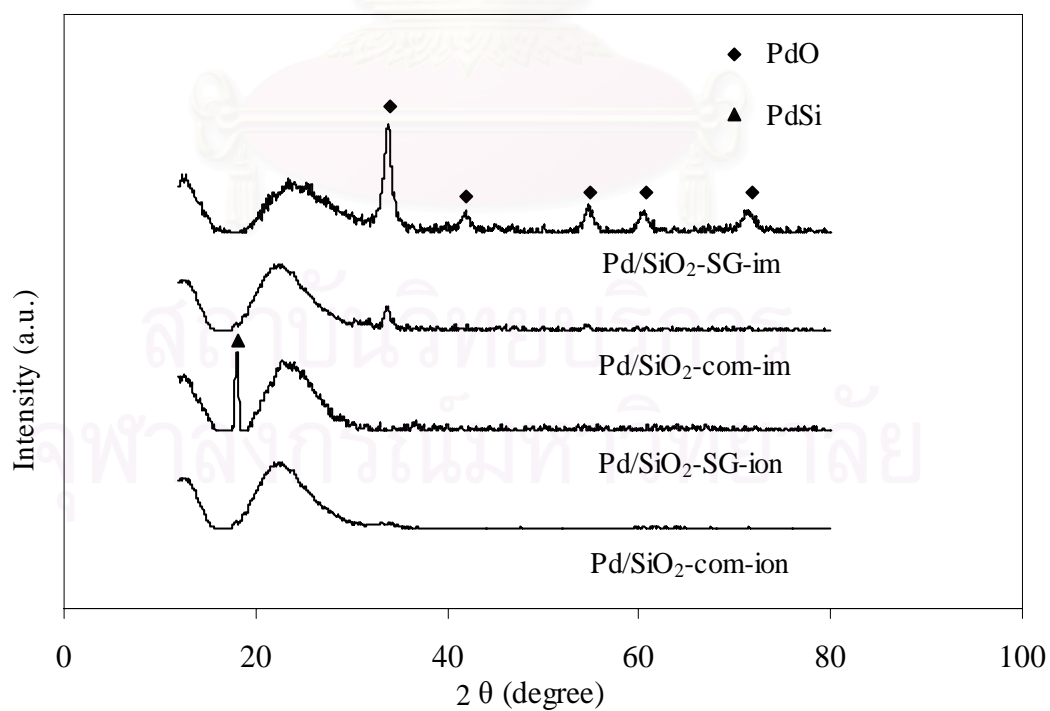
Figure 5.12 XRD patterns of fresh catalysts

5.1.1.5 X-ray Photoelectron Spectroscopy (XPS)

Surface compositions of the catalysts were analyzed using a Kratos Amicus X-ray photoelectron spectroscopy. The XPS analysis were carried out with following conditions: Mg Ka X-ray source at current of 20 mA and 12 keV, resolution 0.1 eV/step, and pass energy 75 eV. The operating pressure is approximately 1×10^{-6} Pa.

A survey scan was performed in order to determine the elements on the catalyst surface. The elemental scan was carried out for C 1s, O 1s, Si 2p and Pd 3d. Binding energies of each element was calibrated internally with carbon C 1s at 285.0 eV. Photoemission peak areas are determined by using a linear routine. Deconvolution of complex spectra are done by fitting with Gaussian (70%)–Lorentzian (30%) shapes using a VISION 2 software equipped with the XPS system.

The percentages of atomic concentration for Si 2p, O 1s and Pd 3d are given in Table 5.3. The atomic ratios of Si/Pd for the sol-gel derived silica supported Pd catalysts prepared by impregnation and ion-exchange method are significantly different that is 19.4 and 215.0, respectively. While those for commercial silica supported Pd catalysts prepared by impregnation and ion-exchange method are 306.2 and 403.0, respectively.

The low Si/Pd ratio found for Pd/SiO$_2$-SG-im catalyst suggests that large amount of palladium existed on the outside of the support surface and not in the pores. The results are consistent with N$_2$ physisorption and XRD results that the average pore diameters remained unaltered (~ 1.9 nm before and after Pd impregnation as shown in Table 5.1). It should be noted that the average PdO crystallite size on SiO$_2$-SG-im calculated from Scherrer equation was much larger than the average pore diameter of sol-gel derived silica. It indicates that PdO could hardly penetrate pores and it formed primarily outer surface. The higher Si/Pd ratios for the others catalysts suggest that most of the palladium existed deep inside the pore of supports more than on the outer surface. This could be the case for the large pore commercial silica supported ones since the pores were large enough so that the solution of Pd precursor could easily be absorbed during the preparation using either impregnation or ion-

exchange method. However, for the sol-gel derived silica, the pores were so small that the preparation solution could hardly penetrate these pores. The enrichment of Si component on the surface of the Pd/SiO_2-SG-ion was due to palladium silicide formation as shown earlier in its XRD pattern. The results were in accordance to those reported by Tschan *et.al* for amorphous $Pd_{81}Si_{19}$ alloy catalysts.

The elemental scans for each component on the surfaces of the silica, the silica supported Pd catalysts prepared by impregnation and ion-exchange are shown in Figure 5.13-5.15, respectively. For silica supports, it was found that the binding energies of both Si 2p and O 1s for the sol-gel derived silica shifted towards lower binding energies. Such results suggest that the sol-gel derived silica has some defects or non-stoichiometric SiO_x ($0<x<2$) (Ichinohe *et al.*). As mentioned in Min *et al.* study it is suggested that the point defects on silica-SG are primary mechanism for inter-diffusion of Pd and then palladium silicide was formed. For the case of the Pd/SiO_2 prepared by impregnation method, the binding energies of Si 2p and O 1s for both Pd/SiO_2-SG-im and Pd-SiO_2-com-im had no changes. Furthermore the binding energies of Pd 3d of both catalysts were also identical. These results indicate that there was no interaction between Pd and silica supports when using impregnation method to prepare the catalysts. On the other hand, for the catalysts prepared by ion-exchange method, the binding energies of Si 2p, O 1s and Pd 3d for Pd/SiO_2-SG-ion shifted towards higher binding energies. The binding energy of Pd 3d for the Pd/SiO_2-SG-ion was significantly increased from that of Pd/SiO_2-com-ion by almost 0.5 eV suggesting that there were strong interaction between Pd and SiO_2 due to palladium silicide formation.

Table 5.3 Atomic concentrations of catalysts from XPS

Catalyst	Atomic Concentration (%)			Si/Pd
	Si 2p	O 1s	Pd 3d	
Pd/SiO$_2$-SG-im	24.06	74.49	1.45	19.4
Pd/SiO$_2$-com-im	21.44	78.49	0.07	306.2
Pd/SiO$_2$-SG-ion	25.80	74.09	0.12	215
Pd/SiO$_2$-com-ion	28.21	71.60	0.08	403.0
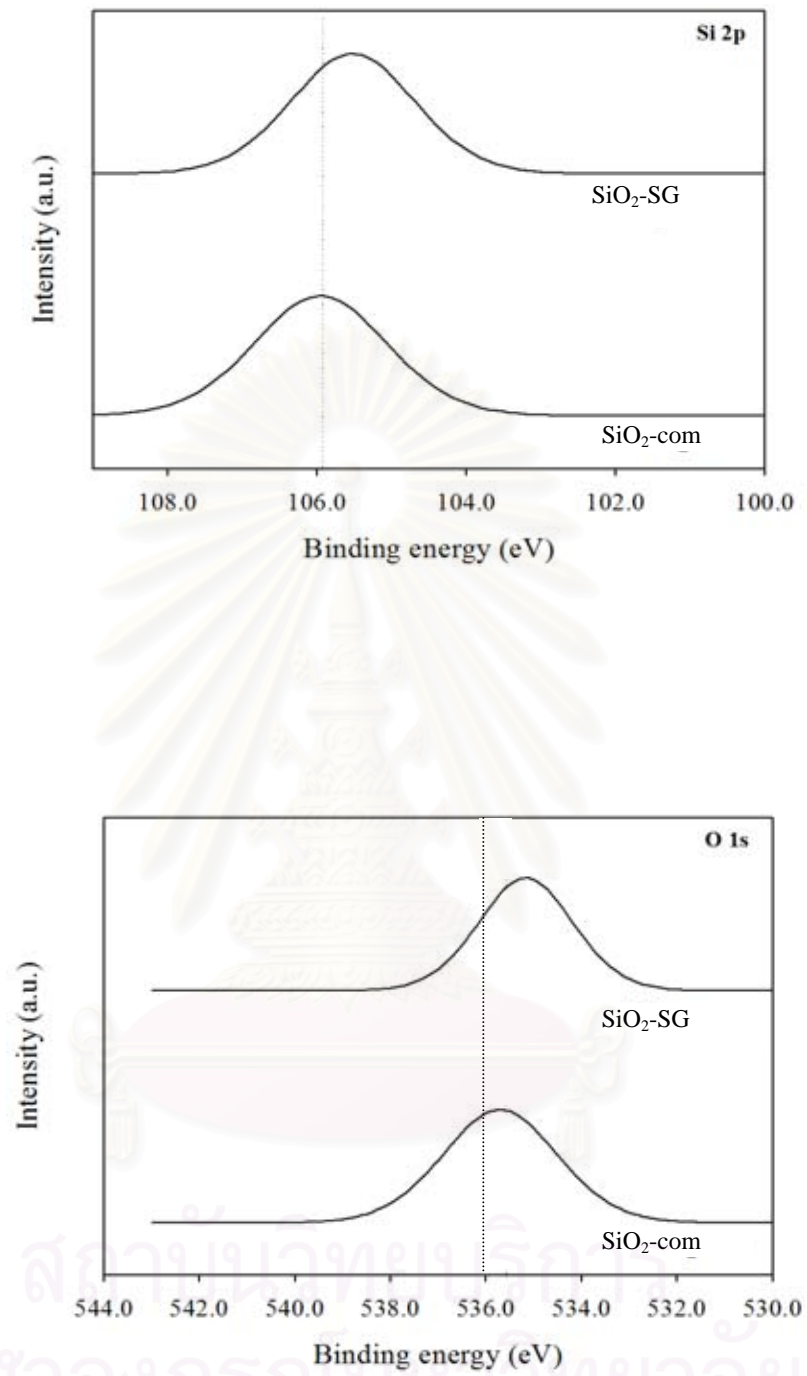
Figure 5.13 XPS results of SiO_2-nano and SiO_2-com
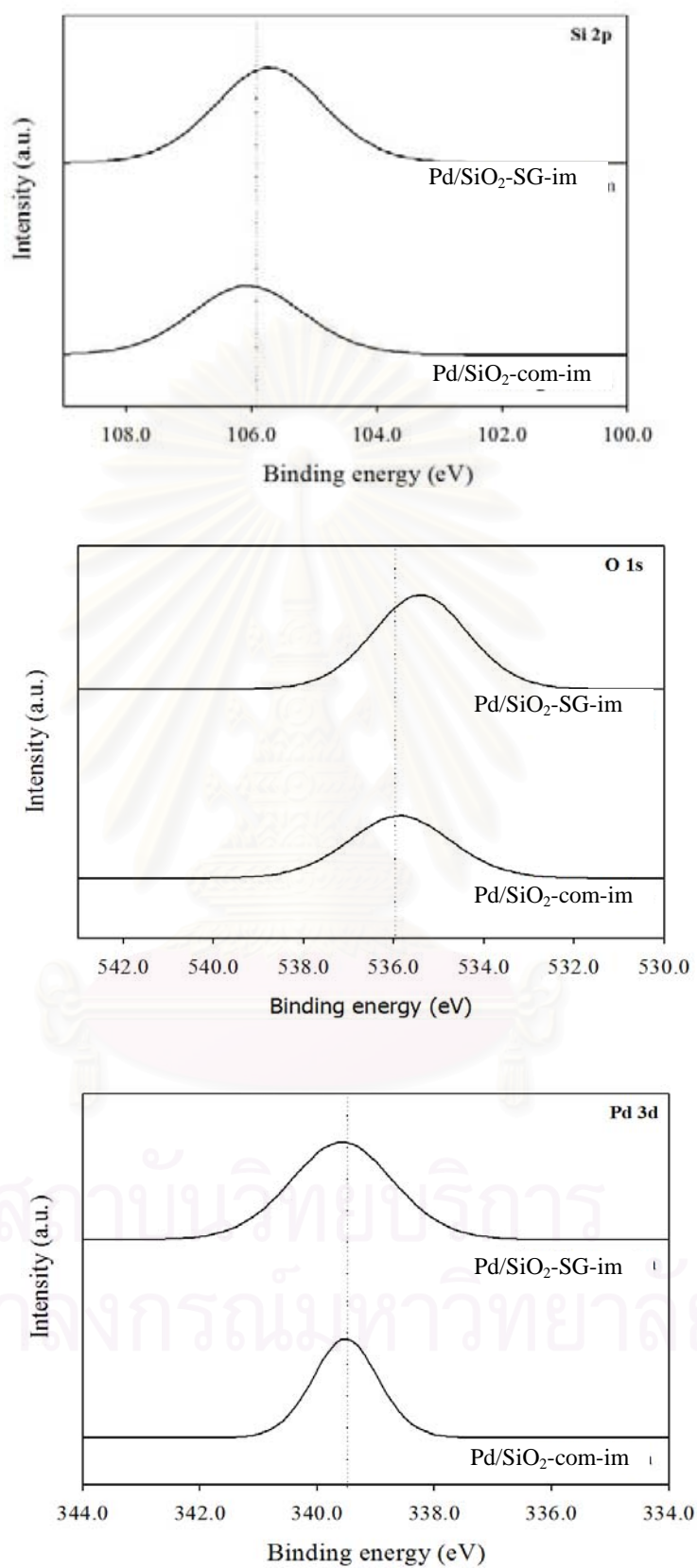
Figure 5.14 XPS results of Pd/SiO$_2$-SG-im and Pd/SiO$_2$-com-im
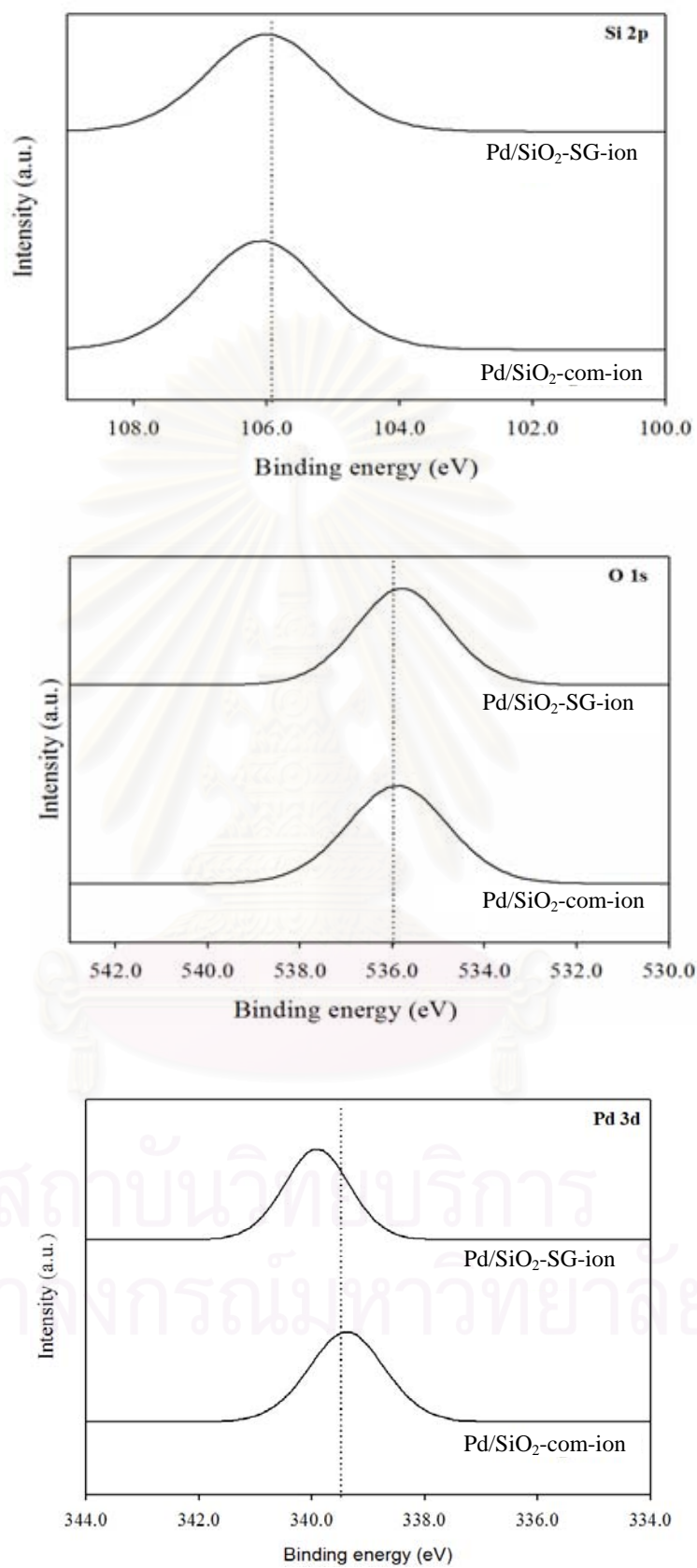
Figure 5.15 XPS results for Pd/SiO$_2$-SG-ion and Pd/SiO$_2$-com-ion

5.1.1.7 CO-Pulse Chemisorption

Chemisorption is the relatively strong, selective adsorption of chemically reactive gases on available metal sites or metal oxide surfaces at relatively higher temperatures (i.e. 25-400°C); the adsorbate-adsorbent interaction involves formation of chemical bonds and heats of chemisorption in the order of 50-300 kJ mol^{-1}.

Since H_2 chemisorption on Pd bridge bonding may occur so there is no precise ratio of atom to Pd metal surface. H/Pd stiochiometry may be varied from 1, 1/2 or 1/3. However, for CO chemisorption, CO/Pd stiochiometry is normally equal to 1. Exposed active surface areas of Pd of the catalysts were calculated from the irreversible pulse CO chemisorption technique based on the assumption that one carbon monoxide molecule adsorbs on one palladium site (Mahata and Vishwanathan, Ali and Goodwin, Sales *et al.*, Sarkany *et al.*, and Nag). The amounts of CO chemisorption on the catalysts are given in Table 5.4. The amounts of CO chemisorption on Pd/SiO$_2$ catalyst increase in the order of Pd/SiO$_2$-com-ion $\gg$ Pd/SiO$_2$-SG-im > Pd/SiO$_2$-SG-ion $\approx$ Pd/SiO$_2$-com-im. As given in Table 5.4, the amounts of CO chemisorption of Pd/SiO$_2$-com-ion are significantly higher than the other catalysts due to its high dispersion of palladium. Comparing the BET surface areas of the original supports, silica-SG has higher surface area than silica-com. For catalysts prepared by impregnation method, the amounts of CO chemisorption are proportional to BET surface area that is active sites increased with increasing BET surface area. The active sites of Pd/SiO$_2$-SG-ion catalyst should be high because it was prepared by ion-exchange method that providing excellent Pd dispersion. But according to Table 5.4, active sites of Pd/SiO$_2$-SG-ion are lower than expectation. It may be caused by palladium silicide formation which is less active than PdO.

Table 5.4 CO- pulse chemisorption results

Catalyst	active site $(\times 10^{-18}$ site/g catalyst)
Pd/SiO$_2$-SG-im	7.41
Pd/SiO$_2$-com-im	3.32
Pd/SiO$_2$-SG-ion	3.92
Pd/SiO$_2$-com-ion	46.80

5.1.2 Reaction Study in Phenylacetylene Hydrogenation

The catalytic properties of the catalysts prepared by two different methods were investigated in phenylacetylene hydrogenation. The reaction was carried out in ethanol solvent at 30°C and 1 bar H_2 pressure. The substrate/ethanol ratio was 1/9. The products are analyzed by gas chromatography with flame ionization (GC-FID) using GS-alumina column.

Hydrogenation activity and selectivity of all the catalysts are presented in Table 5.5. The hydrogenation activities of the catalyst were found to be in the order Pd/SiO$_2$-com-ion > Pd/SiO$_2$-SG-im > Pd/SiO$_2$-SG-ion > Pd/SiO$_2$-com-im which was coincident with the amounts of CO chemisorption. It can be seen that Pd/SiO$_2$-com-ion provided the highest conversion compared to the others catalysts. However the conversion of phenylactylene for Pd/SiO$_2$-com-ion is not remarkable high compared to its significantly high active sites. The turnover of frequencies (TOFs) were calculated using the number of surface metal atoms measured by CO-chemisorption and are given in Table 5.6. The TOFs of Pd/SiO$_2$-SG-im, Pd/SiO$_2$-com-im and Pd/SiO$_2$-SG-ion were 1.05, 1.43, and 1.56 s^{-1}, respectively. While the TOF of Pd/SiO$_2$-com-ion was only 0.18 s^{-1}. According to previous studies (Marin-Astorga *et al.*) it is suggested that changes in the metal dispersion, i.e. different particle sizes, lead also to changes in TOF and selectivity. Furthermore it has been reported that the specific activity decreased with decreasing metal particle size (Molnar *et al*., Duca *et al*., Carturan *et al*., Sarkany *et al*., Albers *et al*., Angel *et al*.), whereas others found that the TOF increased upon increasing the metal dispersion (Duca *et al*.). Such results are consistent with this work that the TOF of Pd/SiO$_2$-com-ion was less than those of the other catalysts due to its higher dispersion and smaller PdO crystallite size. According to Table 5.5, it was found that styrene selectivity of the Pd catalysts supported on the sol gel-derived silica prepared by both methods was higher than those supported on the commercial silica. However it cannot be seen the obvious difference so it is difficult to compare the performance of these catalysts under these reaction conditions.

For a better comparison of the catalysts performance, the reaction conditions were changed to produce the performance curve of the catalysts. As shown in Figure 5.16 the styrene selectivity of all catalysts at low conversion was similar. But when phenylactylene conversion increased styrene selectivity became different. The Pd catalysts supported on the sol-gel derived silica prepared by both methods exhibited better performances compared to those supported on commercial silica with the Pd/SiO$_2$-SG-ion showed the highest styrene selectivity at 100% conversion. Both of the commercial supported Pd catalysts (Pd/SiO$_2$-com-im and Pd/SiO$_2$-com-ion) exhibited no styrene selectivity at such conditions.

Table 5.5 Results of phenylacetylene hydrogenation

Catalyst	Conversion	Selectivity	
		to styrene	to ethylbenzene
Pd/SiO$_2$-SG-im	51.08	96.0	4.0
Pd/SiO$_2$-com-im	31.20	91.1	8.9
Pd/SiO$_2$-SG-ion	40.06	92.9	7.1
Pd/SiO$_2$-com-ion	54.84	88.5	11.5

Table 5.6 TOFs of Pd/SiO$_2$ catalysts

Catalyst	ToF (s^{-1})
Pd/SiO$_2$-SG-im	1.05
Pd/SiO$_2$-com-im	1.43
Pd/SiO$_2$-SG-ion	1.56
Pd/SiO$_2$-com-ion	0.18
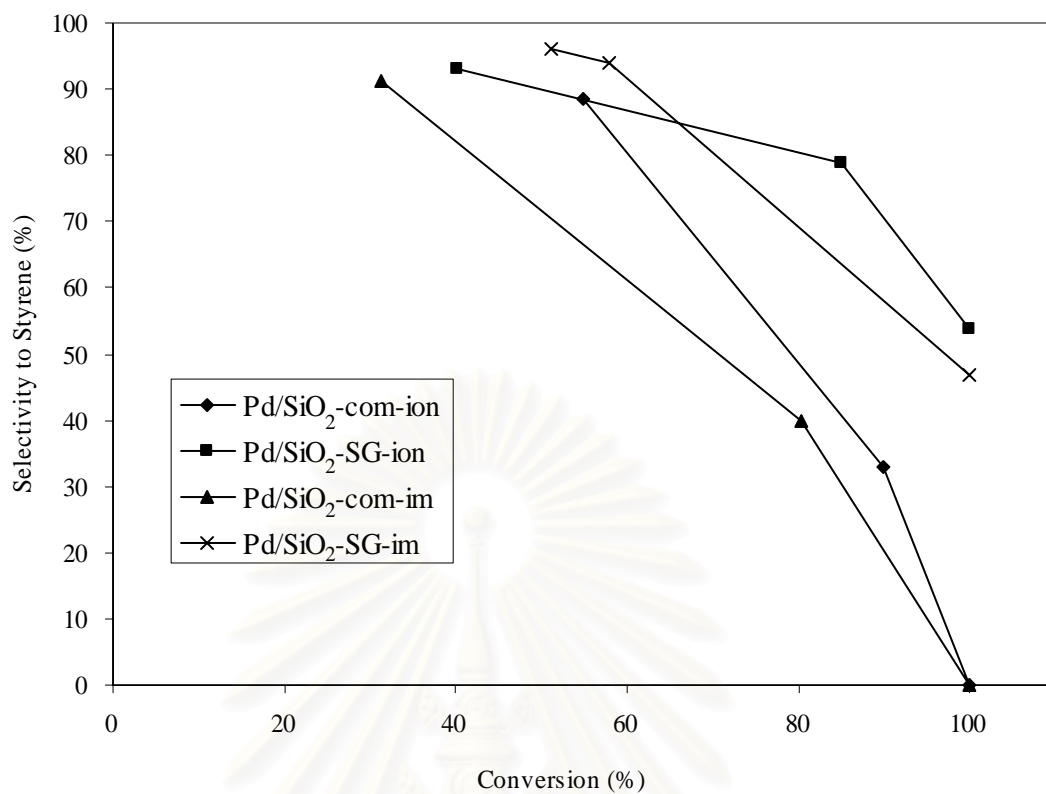
Figure 5.16   Performance curve of Pd/SiO$_2$ catalyst in phenylacetylene

hydrogenation

5.1.3 Catalyst Deactivation

Catalyst deactivation due to metal sintering was studied using XRD technique. After reactions, the catalysts were re-calcined at 450°C for 3 hrs in order to remove carbon deposit and any solvents and were denoted as spent catalysts. According to Figure 5.17 the diffraction peaks for PdO are now evident at $2\theta = 33.8^{o}$, 42.0^{o}, 54.8^{o}, 60.7^{o} and 71.4^{o} for all the spent catalysts, showing that the metal sintering occurred during the liquid phase hydrogenation reaction. The PdO crystallite sizes of Pd/SiO$_2$-SG-im, Pd/SiO$_2$-com-im, Pd/SiO$_2$-SG-ion and Pd/SiO$_2$-com ion were 9.71, 11.72, 5.45 and 4.90, respectively as shown in Table 5.7. It was revealed that the catalyst deactivation due to metal sintering of catalysts prepared by impregnation method was less than those prepared by ion-exchange method. In the case of Pd/SiO$_2$-SG-ion the diffraction peak of palladium silicide was still observed with lower intensity.

Table 5.7 Phases presented and crystallite sizes of spent catalysts

Catalyst	XRD	
	phase	crystallite size of spent catalyst (nm)
Pd-SG-im	PdO	9.71
Pd-com-im	PdO	11.72
Pd-SG-ion	PdSi/PdO	23.49/5.45
Pd-com-ion	n.d.	4.90
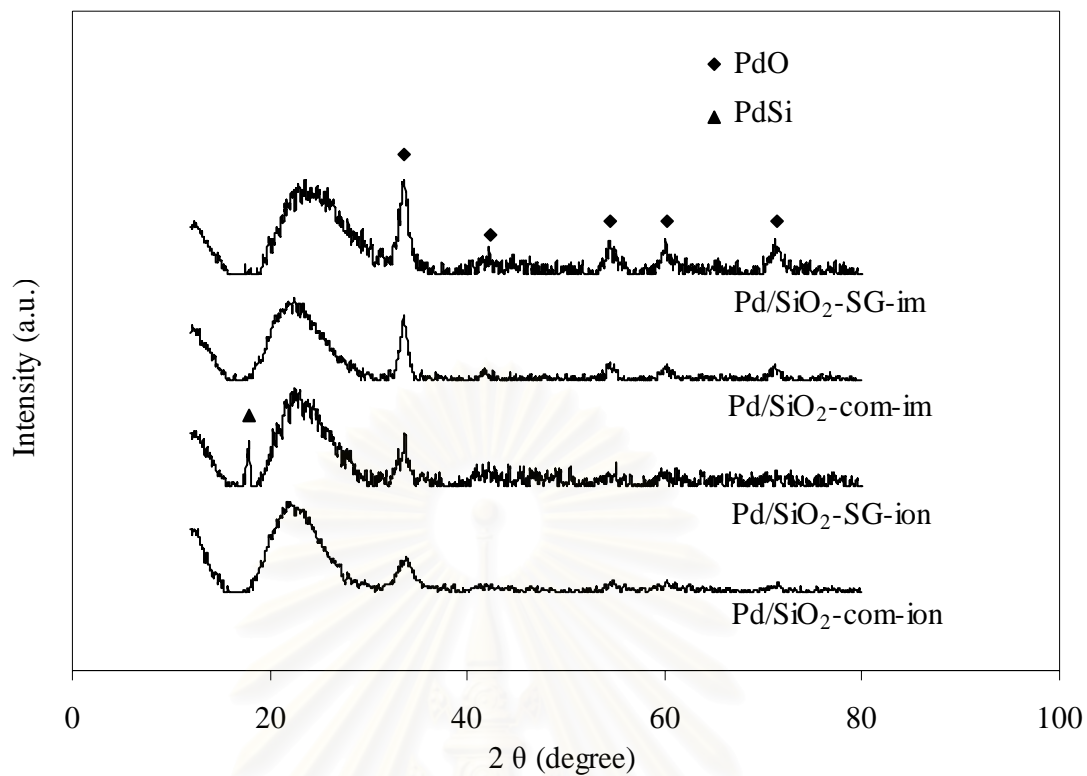
Figure 5.17 XRD patterns of spent catalysts

5.1.4 Effects of calcination temperature and percentage of palladium loading on the characteristics of Pd/SiO$_2$-SG catalysts

In this section, effects of calcinations temperature and percentage of palladium loading on the characteristics of Pd/SiO$_2$-SG catalysts were investigated. The silica were calcined at 300, 500, and 700 and are referred as SiO$_2$-SG-300, SiO$_2$-SG-500, and SiO$_2$-SG-700, respectively. Pd loadings were varied in the range 0.5-10% by weight.

5.1.4.1 N$_2$ Physisorption

BET surface areas, pore volumes and pore diameters of the silica with various sizes were determined by N$_2$ physisorption technique and are shown in Table 5.8. It is shown that BET surface areas and pore volumes of SiO$_2$-SG-300 and SiO$_2$-SG-500 are slightly different whereas those of SiO$_2$-SG-700 dramatically decreased due to thermal sintering. It is suggested that sol-gel derived silica was stable up to 500° C however there were no significant change in the average pore diameters of these three silica.

Table 5.8 N$_2$ physisorption properties of sol-gel derived silica at various calcinations temperature.

Sample	N$_2$ physisorption		
	BET surface area (m^2/g)	Pore Volume (cm^3/g)	Avg Pore Diameter(nm)
SiO$_2$-SG-300	340.1	0.162	1.90
SiO$_2$-SG-500	307.2	0.145	1.89
SiO$_2$-SG-700	44.2	0.022	2.01

5.1.4.2 X-ray diffraction (XRD)

The XRD patterns of the various Pd/SiO_2 prepared by impregnation and ion-exchange method in the calcined state are shown in Figure 5.18 and 5.19, respectively. The XRD characteristic peaks for PdO at 2θ of ca. 33.8 and less so at 42.0, 54.8, 60.7, and 71.4^o were observed only for the catalysts prepared by impregnation method. The average PdO crystallite sizes on SiO_2-SG-300-im, SiO_2-SG-500-im and SiO_2-SG-700-im were calculated from the full width at half maximum of the XRD peak at 33.8^o 2θ using Scherrer's equation (Klug and Alexander) to be 7.6, 9.6 and 13.5 nm, respectively and are given in Table 5.9. It is shown that the cryatallite size of PdO decreased with increasing BET surface areas. For the catalysts prepared by ion-exchange method, it was found that palladium silicide was formed as indicated by XRD characteristic peaks at $2\theta = 18.1^o$. The average palladium silicide crystallite size on SiO_2-SG-300-ion, SiO_2-SG-500-ion and SiO_2-SG-700-ion were calculated to be 98.5, 61.2, and 34.0 nm, respectively as reported in Table 5.9. It is indicated that the average palladium silicide crystallite size decreased with decreasing BET surface areas.

Table 5.9 Phases presented and crystallite sizes of various sol-gel derived silica

supported Pd catalysts

Catalyst	XRD	
	phase	crystallite size (nm)
Pd/SiO$_2$-SG-300-im	PdO	7.6
Pd/SiO$_2$-SG-500-im	PdO	9.6
Pd/SiO$_2$-SG-700-im	PdO	13.5
Pd/SiO$_2$-SG-300-ion	PdSi	98.5
Pd/SiO$_2$-SG-500-ion	PdSi	61.2
Pd/SiO$_2$-SG-700-ion	PdSi	34.0
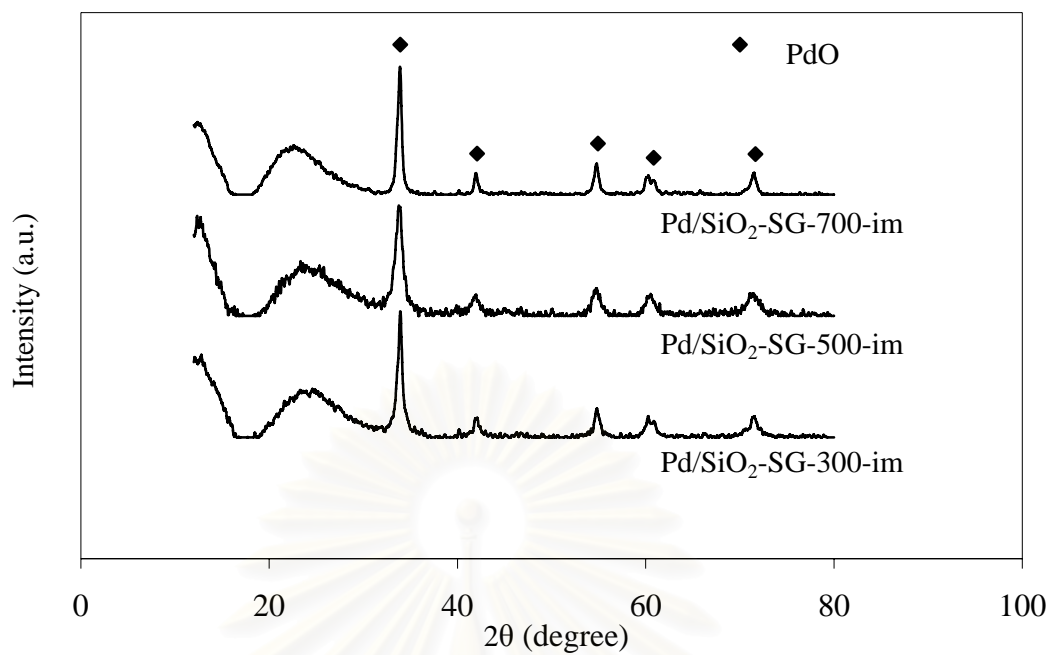
Figure 5.18 XRD patterns of various sol-gel derived silica supported Pd catalysts

prepared by impregnation method
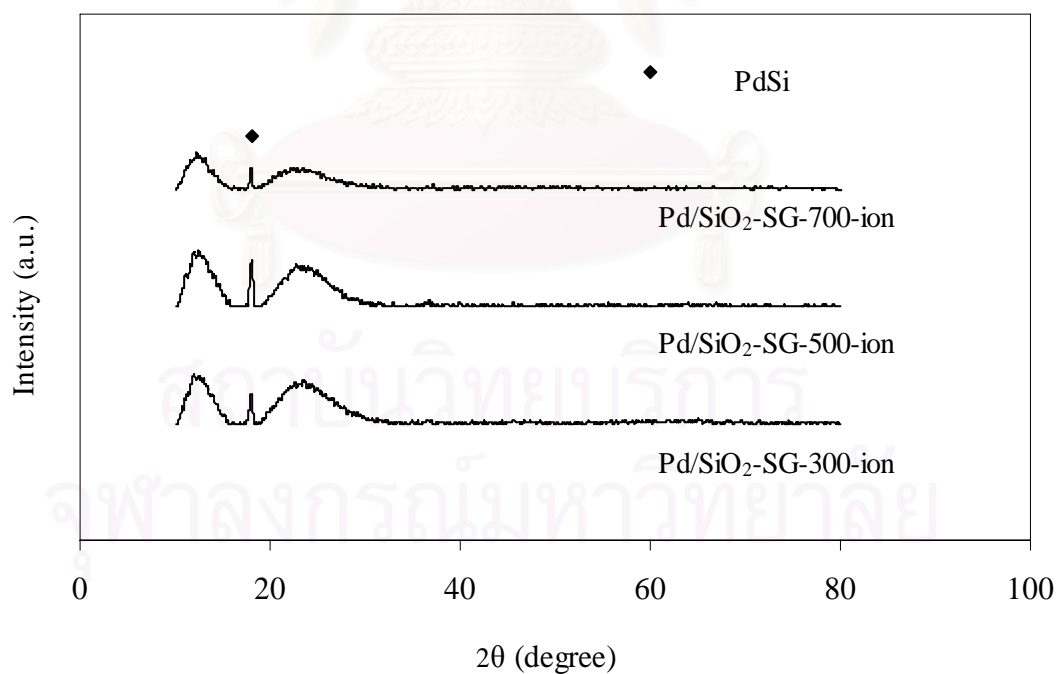
Figure 5.19 XRD patterns of various sol-gel derived silica supported Pd catalysts

prepared by ion-exchange method

5.1.4.3 X-ray Photoelectron Spectroscopy (XPS)

The percentages of atomic concentration for Si 2p, O 1s and Pd 3d are given in Table 5.10. The atomic ratios of Si/Pd for various sizes of the sol-gel derived silica supported Pd catalysts prepared by impregnation and ion-exchange method are significantly different. According to Table 5.10, the atomic ratios of Pd catalysts prepared by ion-exchange method are very high compared to those prepared by impregnation method. As mentioned above in section 5.1.1.5, the high atomic ratios of Si/Pd for Pd catalysts prepared by ion-exchange method were due to palladium silicide formation. It should be noted that the average PdO crystallite size on SiO_2-SG-300-im, SiO_2-SG-500-im, and SiO_2-SG-700-im calculated from Scherrer equation were much larger than the average pore diameters of their original supports resulted in low Si/Pd ratios.

The elemental scan for each component on the surfaces for the various sizes of silica is shown in Figure 5.20. It was found that the binding energies of both Si 2p and O 1s for the sol-gel derived silica calcined at different temperature were not different.

Table 5.10 Atomic concentrations of catalysts from XPS

Catalyst	Atomic concentration (%)			Si/Pd
	Si 2p	O 1s	Pd 3d	
Pd/SiO$_2$-SG-300-im	23.03	74.80	2.18	10.5
Pd/SiO$_2$-SG-500-im	24.06	74.50	1.44	16.7
Pd/SiO$_2$-SG-700-im	17.02	76.03	6.95	2.5
Pd/SiO$_2$-SG-300-ion	29.09	70.82	0.10	290.9
Pd/SiO$_2$-SG-500-ion	25.80	74.09	0.12	215.0
Pd/SiO$_2$-SG-700-ion	28.30	71.51	0.19	148.9
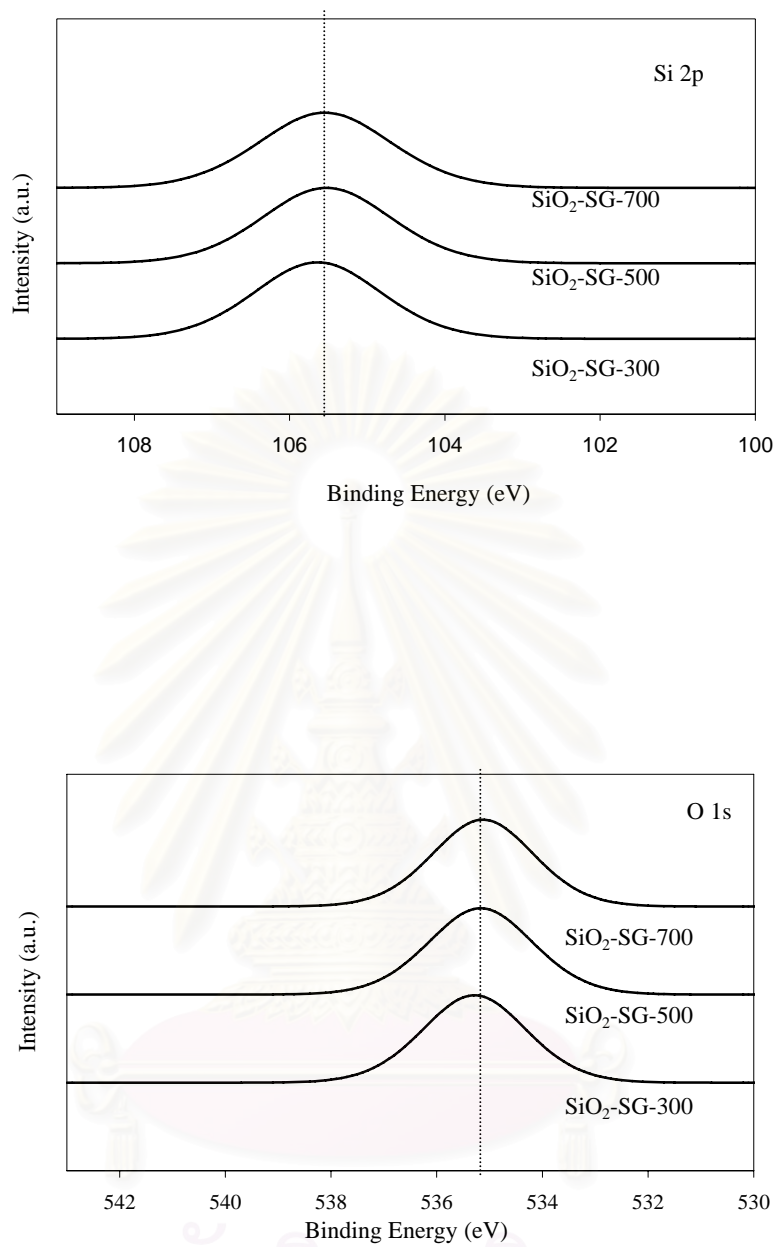
Figure 5.20 XPS results of various sizes of SiO₂

5.1.4.4 CO-Pulse Chemisorption

The amounts of CO chemisorption on the catalysts are given in Table 5.11. Comparing the original supports, BET surface area increased in the order of SiO_2-SG-700 < SiO_2-SG-500 < SiO_2-SG-300. For catalysts prepared by impregnation method, the amounts of CO chemisorption are proportional to BET surface area that is active sites increased with increasing BET surface area. In the case of using ion-exchange method, the amounts of CO chemisorption for Pd/SiO_2-SG-300-ion, Pd/SiO_2-SG-500-ion, and Pd/SiO_2-SG-700-ion are 0.38, 3.92, and 0.00 x10^{18} site/g catalyst, respectively. The lower active sites of Pd catalysts prepared by ion-exchange method compared to those prepared by impregnation method were due to palladium silicide formation which is less active than PdO.

Table 5.11 CO- pulse chemisorption results

Catalyst	active site ($x10^{-18}$ site/g catalyst)
Pd/SiO_2-SG-300-im	14.57
Pd/SiO_2-SG-500-im	7.41
Pd/SiO_2-SG-700-im	0.88
Pd/SiO_2-SG-300-ion	0.38
Pd/SiO_2-SG-500-ion	3.92
Pd/SiO_2-SG-700-ion	0.00

5.1.4.5 Sol-gel derived supported Pd catalysts with various percentage of Pd loading

In this study, the sol-gel derived silica supported Pd catalysts prepared by ion-exchange method were varied the percentage of Pd loading to be 0.5, 1, 2, 5, and 10. The XRD patterns of these catalysts are given in Figure 5.21. The characteristic peaks of palladium silicide at $2\theta = 18.1^o$ were only observed for Pd/SiO2-SG-ion which the percentage of Pd loading is 0.5, 1 and 2. No XRD characteristic peak was observed for Pd catalysts which the percentage of Pd loading is 5 and 10 suggesting that the Pd was highly dispersed and its average particle size was smaller than XRD detectable limit. It should be noted that when Pd concentration is high enough (5 %) the palladium silicide was not formed and its characteristics peak is no longer observed. The average palladium silicide crystallite size was calculated to be 0.5 % Pd/SiO$_2$-SG-ion, 1 % Pd/SiO$_2$-SG-ion and 2 % Pd/SiO$_2$-SG-ion to be 53.6, 61.2, and 61.7, respectively as shown in Table 5.12. There were no significant different in the average palladium silicide crystallite size of these three catalyst.

Table 5.21 Phases presented and crystallite sizes of sol-gel derived silica supported Pd catalysts with various percentage of Pd loading

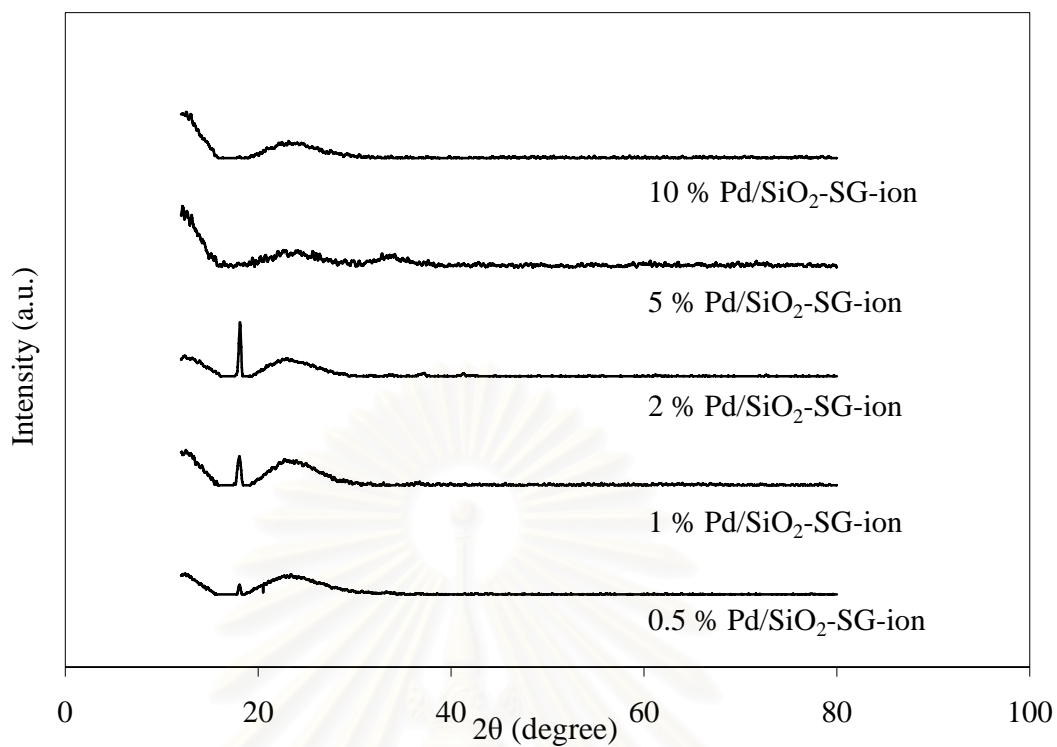| Catalyst	XRD	
	phase	crystallite size (nm)
0.5% Pd/SiO$_2$-SG-ion	PdSi	53.6
1% Pd/SiO$_2$-SG-ion	PdSi	61.2
2% Pd/SiO$_2$-SG-ion	PdSi	61.7
5% Pd/SiO$_2$-SG-ion	n.d.	n.d.
10% Pd/SiO$_2$-SG-ion	n.d.	n.d.

Figure 5.21 XRD patterns of sol-gel derived silica supported Pd catalysts with various

percentages of Pd loading

5.2 Liquid Phase Hydrogenation on Pd/SiO$_2$ in Organic Solvents and Under Pressurized Carbon Dioxide

Liquid-phase hydrogenation of cyclohexene on Pd/SiO$_2$ prepared by ion-exchange method was carried out as a model reaction to compare the effect of solvents. The catalyst deactivations due to metal sintering and metal leaching were investigated using XRD and AAS, respectively.

5.2.1 Liquid Phase Hydrogenation in different solvents

Catalyst activities for liquid phase hydrogenation of cyclohexene at 25°C in various organic solvents, under pressurized carbon dioxide, and under solvent less condition are shown in Table 5.13. In hydrogenation reaction, H$_2$ solubility in common organic solvents is usually low depending on the nature of the solvent. It has been reported that hydrogenation activity decreases with increasing solvent polarity due to competitive adsorption of high polar solvent and substrate on the catalyst surface (Singh and Vannice, and Augustine and Techasauvapak) For organic solvents used in this study, the hydrogenation activities of cyclohexene increased in the order NMP < heptanol< benzene and the cyclohexene conversion was determined to be 15.1, 27.6, and 57.0, respectively. It was found that the catalyst activities increased with decreasing the polarity of solvent as in previous studies. It is obvious that the hydrogenation rates are much higher for those performed in high pressure CO$_2$ than those carried out in organic solvents. However the concentration of either cyclohexene or H$_2$ in high pressure CO$_2$ was different from those in organic solvents, it is not easy to compare the results at 6 MPa CO$_2$ with those in organic solvents. Compared to under solvents less condition the hydrogenation rate increased from 93% to nearly 100% in the presence of high pressure CO$_2$. The results were probably from the higher H$_2$ solubility in CO$_2$ medium.

The effect of CO$_2$ pressure on liquid phase hydrogenation of cyclohexene on Pd/SiO$_2$ catalysts was also investigated for CO$_2$ pressure in the range between 0 and 14 MPa at 40°C where CO$_2$ can be in the supercritical state. As shown in Figure 5.22, it is seen that the hydrogenation rate increases with increasing CO$_2$ pressure. Phase behavior study revealed that the mixture of cyclohexene and CO$_2$ (without catalyst)

was gas-liquid two phases at pressures up to 9 MPa but a single phase at 9.4 MPa or above.   Nearly 100% cyclohexene conversions were observed under those homogeneous conditions. Arai *et al*. has recently suggested that hydrogenation rate in dense carbon dioxide strongly correlates with the phase behavior of the reaction mixture.

Table 5.13 Catalytic activities of Pd/SiO_2 for cyclohexene hydrogenation in various
solvents

Solvent	Polarity	Time (min)	Conversion (%)
NMP	4.09	10	15.1
Heptanol	1.33	10	27.6
Benzene	0.0	10	57.0
Cyclohexene	0.0	2	93.0
		10	96.0
CO_2 6 MPa	0.0	2	~100.0
		10	~100.0
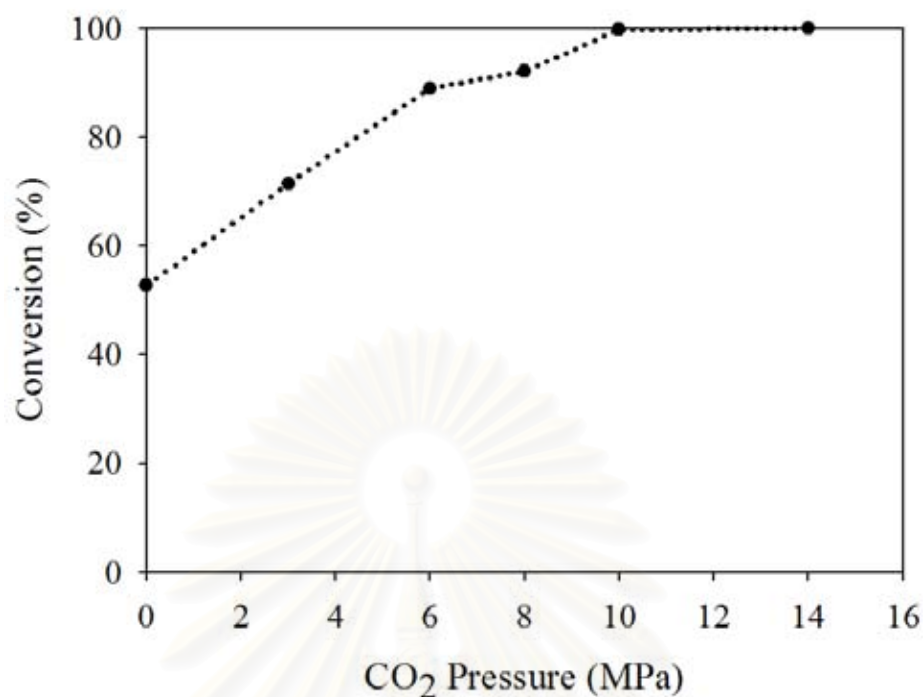
Figure 5.22 Effect of CO_2 pressure on the hydrogenation activities of Pd/SiO$_2$

5.2.2 Characterization of the Catalysts Before and After Liquid Phase Hydrogenation Reaction

5.2.2.1 X-ray diffraction (XRD)

After reactions run, catalyst deactivation due to metal leaching was studied. The XRD patterns of the fresh catalysts (after 1st calcination), after reduction in H$_2$ at room temperature, after reduction and re-calcination (without reaction), and after reduction and being used in hydrogenation reaction with NMP solvent are shown in Figure 5.23. There was no significant change in the XRD patterns of the calcined, the reduced, and the re-calcined catalysts (without reaction) since only a broad peak for SiO$_2$ was observed at $2\theta = 22^o$. XRD characteristic peaks for palladium oxide (PdO) or metallic Pd^0 were not detected, suggesting that palladium was highly dispersed on the silica support and its crystallite size was smaller than the XRD detectable limit. However, XRD characteristic peak for metallic Pd^0 was observed after reduced and

being used in hydrogenation reaction. Therefore, metal sintering did not occur by the reduction at ambient temperature or by thermal effects during the calcination at 450°C. After being subjected to the hydrogenation reaction runs, the catalysts were re-calcined at 450°C for 3 h in order to remove any carbon deposits and solvents. The XRD patterns of these so-called spent catalysts are shown in Figure 5.24. The diffraction peaks for PdO are now evident at $2\theta = 33.8^{o}$, 42.0^{o}, 54.8^{o}, 60.7^{o} and 71.4^{o} for all the spent catalysts, showing that the metal sintering occurred during the liquid phase hydrogenation reaction, since no XRD peak of PdO was detected over the re-calcined catalyst (Figure 5.23). The PdO crystallite sizes were calculated from the full width at half maximum of the XRD peak at $2\theta = 33.8^{o}$ using Scherrer equation and are reported in Table 5.14. The crystallite sizes of PdO on the spent catalysts were in the order of solvent-less < benzene < CO_2 < heptanol < NMP and were calculated to be 3.5, 3.9, 7.6, 10.3 and 11.0 nm, respectively.

Table 5.14 Crystallite sizes of fresh and spent catalysts

Catalyst	PdO particle size (nm)
Fresh	n.d.
Spent-benzene	3.9
Spent-CO_2 6 MPa	7.6
Spent-solvent less	3.5
Spent-heptanol	10.3
Spent-NMP	11.0
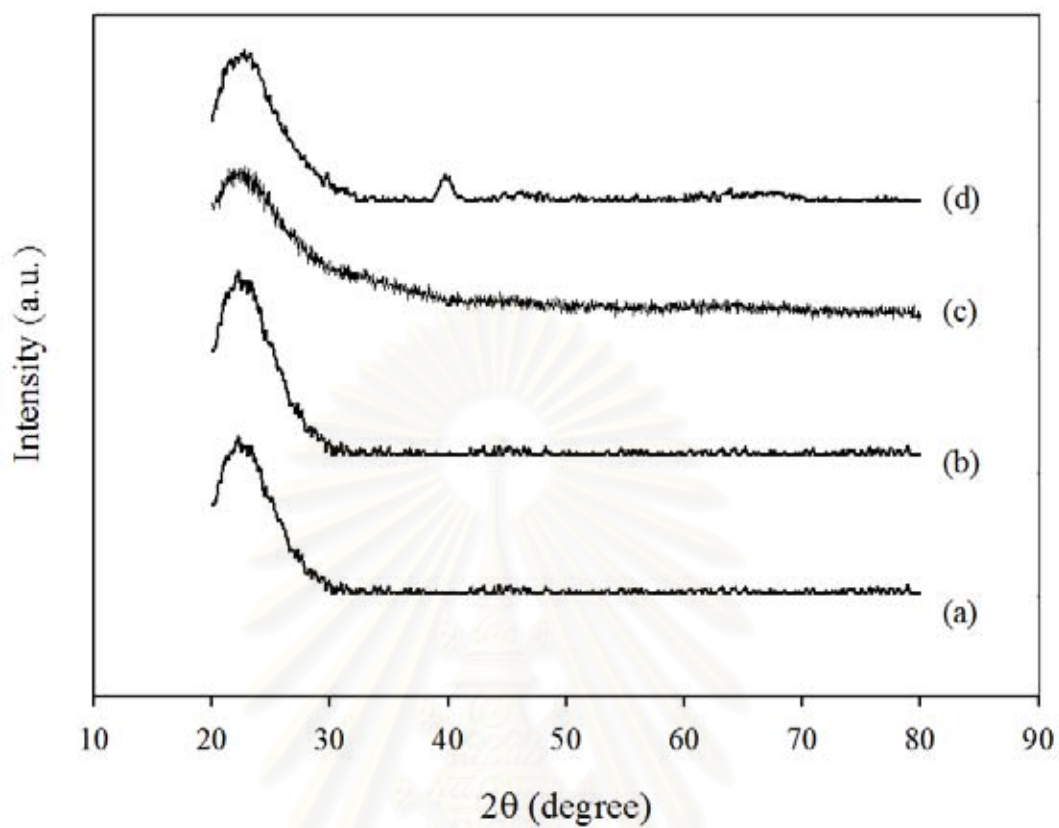
Figure 5.23 XRD patterns of Pd/SiO$_2$ catalysts (a) after 1st calcination and (b) after

reduced in H$_2$ at room temperature (c) after reduced and re-calcination

(without reaction) and (d) after reduced and reaction in NMP.
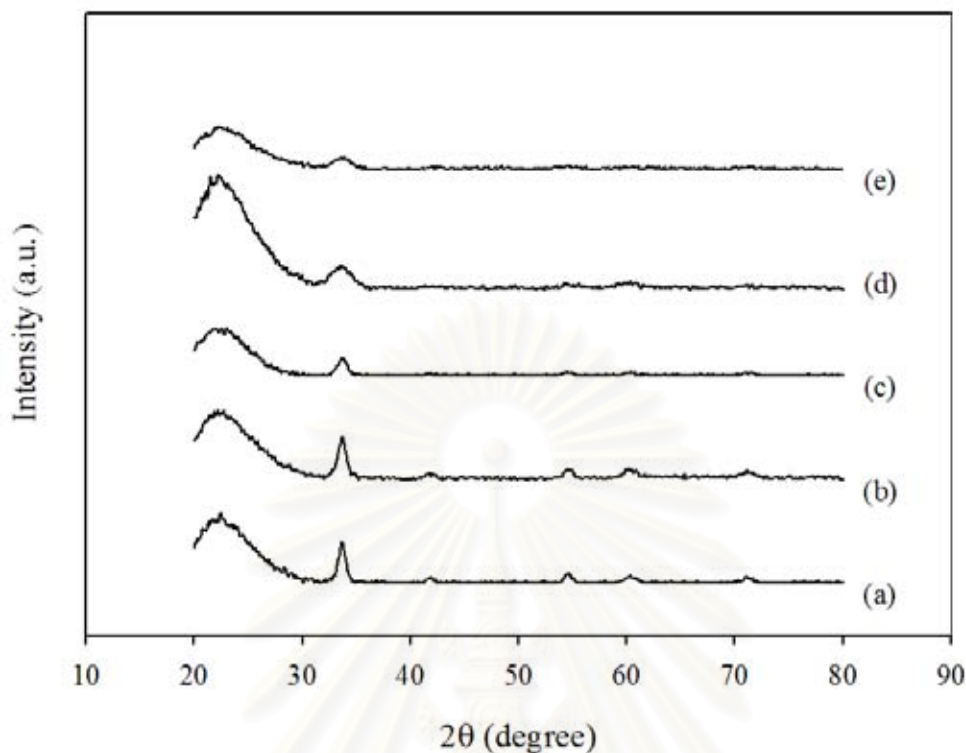
Figure 5.24 XRD patterns of re-calcined spent Pd/SiO$_2$ catalysts after hydrogenation reaction

5.2.2.2 Atomic Absorption Spectroscopy

Atomic absorption spectroscopy is a very common technique for quantitative measurement of atomic composition based on photon absorption of a vaporized aqueous solution prepared from the starting material.

The actual amounts of palladium loading before and after reaction determined by atomic adsorption spectroscopy are given in Table 5.15. The palladium loading on the fresh catalyst is 0.97 wt.% and those on the spent catalysts are always lower than that on the fresh catalyst, meaning that palladium was leached in the course of the reaction. Leaching of active metal is another main cause of catalyst deactivation in liquid phase reaction. In general, it depends upon the reaction medium (pH, oxidation potential, chelating properties of molecules) and upon bulk and surface properties of

the metal (Besson and Gallezot). In this study, the percentages of the leaching are 11.3, 20.6, 12.4, 15.5 and 21.6 in benzene, CO_2, solvent less, heptanol and NMP, respectively.

Table 5.15 The actual amounts of palladium loading and the percentage of Pd leaching

Catalyst	Amount of Pd (wt.%)	Pd leached (%)
Fresh	0.97	–
Spent-benzene	0.86	11.3
Spent-CO_2 6 MPa	0.77	20.6
Spent-solvent less	0.85	12.4
Spent-heptanol	0.82	15.5
Spent-NMP	0.76	21.6

5.2.2.3 CO-pulse chemisorption

The amounts of CO chemisorption for fresh catalyst were calculated based on the assumption that CO/Pd stiochiometry is normally equal to 1. The active sites of fresh catalyst were 2.43×10^{19} molecule/g-cat and the percentage of Pd dispersion was 44.3 as shown in Table 5.16.

After reaction, the amounts of CO chemisorbed, i.e. the number of surface Pd atoms, significantly decreased by 60% or more for all the spent catalysts. The active sites decreased in the order benzene > CO_2 6 MPa > solvent less > heptanol > NMP. The similar trend was observed for the percentage of Pd dispersion. The decreases in the amount of CO adsorbed were much more than those expected from the results for the Pd leaching. This would be caused by the Pd sintering. The Pd dispersions determined for the spent catalysts are below 50% of for the fresh catalyst. The extent of the Pd sintering depends on the solvent employed for the reaction and is significant

in heptanol and NMP. The Pd dispersions of the spent catalysts used in these polar solvents are below 10% of that of the fresh catalyst.

Table 5.16 The amounts of CO chemisorption

Catalyst	Amount of CO chemisorption x 10^{19} (molecule/g-cat.)	Pd Dispersion (%)
Fresh	2.43	44.3
Spent-benzene	1.00	20.6
Spent-CO_2 6 MPa	0.61	14.0
Spent-solvent less	0.38	6.9
Spent-heptanol	0.18	3.9
Spent-NMP	0.16	3.8

CHAPTER VI

CONCLUSIONS AND RECOMMENDATIONS

6.1 Conclusions

In this chapter, the conclusions are divided in two parts as following :

6.1.1 Selective Hydrogenation of Phenylacetylene

1. When the sol-gel derived silica was employed as a support for Pd catalysts, palladium silicide was formed if ion-exchange method was used for catalyst preparation as shown by both XRD and XPS results.

2. Based on the calculated TOFs, it was found that the specific activity decreased as metal particle size decreased (% dispersion increased). The TOFs was very low when the average Pd particle size was smaller than 3-5 nm.

3. The Pd catalysts supported on the sol-gel derived silica prepared exhibited better performances compared to those supported on commercial silica regardless their preparation method.

4. Catalyst deactivation due to metal sintering occurred for those prepared by ion-exchange method.

Liquid Phase hydrogenation on Pd/SiO$_2$ in Organic Solvents and Under pressurized Carbon Dioxide

1. When using organic solvents in cyclohexene hydrogenation, the least polar solvent gave the highest hydrogenation activity.

2. Compared to the use of organic solvents or solvent less, the use of high pressure CO_2 significantly enhanced the hydrogenation activity and the hydrogenation activity increased with increasing the pressure of CO_2.

3. The catalyst deactivations due to metal sintering and metal leaching in the presence of high pressure CO_2 were comparable to those in organic solvents.

6.2 Recommendations

1. The mechanism for deactivation of metal catalyst due to metal leaching and metal sintering during liquid phase hydrogenation should be studied.

2. Selective hydrogenation of phenylacetylene on Pd/SiO_2 in high pressure CO_2 should be investigated.

3. The mechanism for the different behaviors of the Pd catalysts supported on sol-gel silica and commercial silica at high phenylacetylene conversion should be investigated.

REFERENCES

Alber, P., Pietsch, J., and Parker, S.F. Poisoning and deactivation of palladium catalyst. *J. Mol. Catal. A* 173 (2001): 275-286.

Albers, P., Seibold, K., Prescher, G., and Muller, H. XPS and SIMS studies of carbon deposits on Pt/Al$_2$O$_3$ and Pd/SiO$_2$ catalysts applied in the synthesis of hydrogen cyanide and selective hydrogenation of acetylene. *Appl. Catal. A.* 176 (1999): 135-146.

Ali, S.H., and Goodwin, J.G. Investigation of Palladium Precursor and Support effects on CO Hydrogenation over Supported Pd Catalysts. *J.Catal.* 176 (1998): 3–13.

Angel, G. D., and Benitez, J.L. Ammonia and sulfur poisoning effects on hydrogenation of phenylacetylene over Pd supported catalysts. *J. Mol. Catal. A* 94 (1994): 409-416.

Arunajatesan, V., Subramaniam, B., Hutchenson, K. W.,and Herkes, F. E. Fixed-bed hydrogenation of organic compounds in supercritical carbon dioxide. *Chem. Eng. Sci.* 56 (2001): 1363-1369.

Augustine, R.L., Techasauvapak, P. Heterogeneous catalysis organic synthesis part 9. specific site solvent effects in catalytic hydrogenations. *J. Mol. Catal. A* 87 (1994): 95.

Besson, M., and Gallezot, P. Deactivation of metal catalysts in liquid phase organic reactions *Catal. Today* 81 (2003): 547-559.

Burgener, M., Furrer, R., Mallat, T., and Baiker, A. Hydrogenation of citral over Pd/alumina: comparison of "supercritical" CO$_2$ and conventional solvents in continuous and batch reactor *Appl. Catal. A.* 268 (2004): 1-8.

Carturan, G., Facchin, G., Cocco, G., Enzo, S., and Navazio, G. Influence of metal dispersion on selectivity and kinetics of phenylacetylene hydrogenation catalyzed by supported palladium. *J. Catal.* 76 (1982): 405-417.

Dominguez-Quintero, O., Martinez, S., Henrequez, Y., D'Ornelas, L., Krentzien, H., and Osuna, J. Silica-supported palladium nanoparticles show remarkable hydrogenation catalytic activity *J. Mol. Catal. A* 197 (2003): 185-191.

Duca, D., Liotta, L.F., and Deganello, G. Liquid phase hydrogenation of phenylacetylene on pumice supported palladium catalysts. *Catal. Today* 24 (1995): 15-21.

Duca, D., Liotta , L.F., and Deganello, G. Selective Hydrogenation of Phenylacetylene on Pumice-Supported palladium Catalysts. *J. Catal* 154 (1995): 69-79.

Fengyu, Z., Kenji, M., Masayuki, S., and Masahiko, A. Recyclable Homogeneous/Heterogeneous Catalytic Systems for Heck Reaction through Reversible Transfer of Palladium Species between Solvent and Support *J. Catal. A* 194 (2000): 479–483.

Fengyu, Z., Masayuki, S., Yutaka, I., and Masahiko, A. The leaching and re-deposition of metal species from and onto conventional supported palladium catalysts in the Heck reaction of iodobenzene and methyl acrylate in *N*-methylpyrrolidone. *J. Mol.Catal. A* 180 (2002): 211–219.

Fengyu, Z., Yutaka, I., and Masahiko, A. Hydrogenation of nitrobenzene withsupported platinum catalysts in supercritical carbon dioxide: effects of pressure, solvent, and metal particle size *J. Catal.* 224 (2004): 479–483.

Fengyu, Z., Yutaka, I., Maya, C., Osamu, S., and Masahiko, A. Hydrogenation of an α,β-unsaturated aldehyde catalyzed with ruthenium complexes with different fluorinated phosphine compounds in supercritical carbon dioxide and conventional organic solvents. *J. Supercritical Fluids* 27 (2003): 65-72.

Heidenreich, R.G., Krauter, J.G.E., Pietsch, J., and Kohler K. Control of Pd leaching in Heck reactions of bromoarenes catalyzed by Pd supported on activated carbon *J. Mol. Catal. A* 182-183 (2003): 499-509

Ichinohe, T., Masaki, S., Kawasaki, K., and Morisaki, H. Palladium silicide/oxide formations in Pd/SiO$_2$ complex films. *Thin Solid films*. 343-344 (1999): 119-122.

Jackson, S. D., and Shaw, L.A. The liquid phase hydrogenation of phenylacetylene and styrene on palladium/carbon catalyst. *Appl. Catal. A*. 134 (1996): 161-168.

Joice, P.M., and Srinivasan, M. Photoelectron Spectroscopy (XPS) Studies on some Palldium Catalysts. *Eur. Polym. J*. 31 (1994): 835-839.

Klug, H.P., and Alexander, E. "X-Ray Diffraction Procedures For Polycrystalline Amorphous Materials 2nd ed.", Wiley, New York, 1974.

Mahata, N., and Vishwanathan, V. Influence of Palladium Precursors on Structural Properties and Phenol Hydrogenation Characteristics of Supported Palladium. Catalysts. *J. Catal*. 196 (2000): 262–270.

Marin-Astorga, N., Alvez-Manoli, G., Reyes, P. Stereoselective hydrogenation of phenyl alkyl acetylenes on pillared clays supported palladium catalysts. *J. Mol. Catal. A* 226 (2005): 81-88.

Min, B.K., Santra, A.K., and Goodman, D.W. Understanding silica-supported metal catalysts: Pd/silica as a case study *Catal. Today* 85 (2003): 113–124.

Molnar, A., Sarkany, A., and Varga, M. Hydrogenation of carbon–carbon multiple bonds: chemo-, regio- and stereo-selectivity. *J. Mol. Catal. A* 173 (2001): 185-221.

Nag, N. K. A study on the dispersion and catalytic activity of gamma alumina supported palladium catalysts. *Catal. Lett.* 24 (1994): 37-46.

Nozoe, T., Tanimoto, K., Takemitsu, T., Kitamura, T., Harada, T., Osawa, T. and Takayasu, O. Non-solvent hydrogenation of solid alkenes and alkynes with supported palladium catalyst. *Solid State Ionics* 141 (2001): 695-700.

Palinko, I. Effects of surface modifiers on the liquid-phase hydrogenation of alkenes over silica-supported platinum, palladium and rhodium *Appl. Catal. A*. 126 (1995): 39-49.

Panpranot, J., Pattamakomsan, K., Praserthdam, P. and Goodwin, G.J. A comparative study of Pd/SiO$_2$ and Pd/MCM-41 catalysts in liquid-phase hydrogenation. *Catal. Com.* 5 (2004): 583-590.

Panpranot, J., Pattamakomsan, K., Praserthdam, P. and Goodwin, G.J. Impact of the silica support structure on liquid phase hydrogenation on Pd catalysts. *Ind. Eng. Chem. Res.* 43 (2004): 6014-6020.

Pillai, U.R., Sahle-Demessie, E. Hydrogenation of 4- Oxoisophorone over a Pd/Al$_2$O$_3$ catalyst under supercritical CO$_2$ medium. *Ind. Eng. Chem. Res.* 42 (2003): 6688-6696.

Pillai, U.R., Sahle-Demessie, E., and Young, D. Maleic anhydride hydrogenation over Pd/Al$_2$O$_3$ catalyst under supercritical CO$_2$ medium *Appl. Catal. B.* 43 (2003): 131-138.

Rylander, P.N., "Hydrogenation Methods", (1985a).

Rylander, P.N., Hydrogenation Olefins, in "Hydrogenation Methods", (1985b).

Sales, E.A., Bugli, G., Ensuque, A., Mendes, M.J., Bozon-Verduraz, F. Palladium Catalysts in the Selective Hydrogenation of Hexa-1,5-diene and Hexa-1,3-diene in the Liquid Phase. Effect of Tin and Silver Addition-Part 1.

Preparation and Characterization: From the Precursor Species to the Final Phases. *Chem. Phys.* (1999): 491-498.

Sarkany, A., Weiss, A.H., and Guczi, L. Structure sensitivity of acetylene-ethylene hydrogenation over Pd catalysts**.** *J. Catal.* 98 (1986): 550-553.

Sarkany, A., Zsoldos, Z., Furlong, B., Hightower, J. W., and Guczi, L. Hydrogenation of 1-Butene and 1,3-Butadiene Mixtures over Pd/ZnO Catalysts. *J. Catal.* 141 (1993): 566-582.

Schmid, L., Schneider, M.S., Engel, D., and Baiker, A. Formylation with "supercritical" CO2: Efficient ruthenium-catalyzed synthesis of N-formylmorpholine. *Catal. Lett.* 88 (2003): 105-113**.**

Shin-ichiro, F., Shuji, A., Fengyu, Z., Ruixia, L., Masashi, H., and Masahiko, A. Selective hydrogenation of cinnamaldehyde using ruthenium–phosphine complex catalysts with multiphase reaction systems in and under pressurized carbon dioxide: Significance of pressurization and interfaces for the control of selectivity. *J. Catal.* 236 (2005): 101–111.

Singh, U.K., and Vannice M.A. Kinetic and thermodynamic analysis of liquid-phase benzene hydrogenation. *AIChE J.* 45 (1999): 1059-1071**.**

Singh, U.K., and Vannice M.A. Liquid-phase citral hydrogenation over SiO_2-supported group VIII metals *J. Catal.* 199 (2001): 73-84.

Stanger, K.J., Tang, Y., Andereg, J., and Angelici, R.A. Arene hydrogenation using supported rhodium metal catalysts prepared from $[Rh(COD)H]_4$, $[Rh(COD)_2]^+BF^{4-}$, and $[Rh(COD)Cl]_2$ adsorbed on SiO_2 and Pd-SiO_2 *J. Mol. Catal. A.* 202 (2003): 147–161.

Tanaka, S., Mizukami, F., Niwa, S., Toba, M., Maeda, K., Shimada, H., and Kunimori, K. Preparation of highly dispersed silica-supported palladium catalysts by complexing agent-assisted sol-gel method and their characteristics. *Appl. Catal. A.* 229 (2002): 165-174.

Tschan, R., Wandeler, R., Schneider, M.S., Burgener, M., Schubert, M.M., and Baiker, A. Continuous Semihydrogenation of Phenylacetylene over Amorphous $Pd_{81}Si_{19}$ Alloy in "Supercritical" Carbon Dioxide: Relation between Catalytic Performance and Phase Behavior. *J. Catal.* 204**,** (2001): 219–229.

Tschan, R., Wandeler, R., Schneider, M.S., Burgener, M., Schubert, M.M., and Baiker, A. Semihydrogenation of a propargylic alcohol over highly active amorphous

Pd$_{81}$Si$_{19}$ in "supercritical" carbon dioxide. *Appl. Catal. A.* 223 (2002): 173–185.

Wandeler, R., Kunzle, N., Schneider, M. S., Mallat, T., and Baiker, A. Continuous Enantioselective Hydrogenation of Ethyl Pyruvate in "Supercritical" Ethane: Relation between Phase Behavior and Catalytic Performance. *J. Catal.* 200 (2000): 377–388.

Yamada, H. and Goto, S. The effect of solvents polarity on selective hydrogenation of unsaturated aldehyde in gas-liquid-solid three phase reactor *J. Chem. Eng. Japan* 36 (2003): 586-589.

Yuriko, N., Takeshi, K., and Yasuaki, O. Solvent effect on the structure sensitivity in enantioselective hydrogenation of (, β-unsaturated acids with modified palladium catalysts *J. Mol. Catal. A* 212 (2004): 155–159.

APPENDICES

APPENDIX A

CALCULATION FOR CATALYST PREPARATION

Preparation of 1%Pd/SiO$_2$ catalysts by the incipient wetness impregnation and ion-exchange method are shown as follows:

Reagent: - Tetraammine Palladium(II)chloride monohydrate (98%)

        Molecular weight. = 263.44

     - Support: SiO$_2$

Example Calculation for the preparation of 1%Pd/SiO$_2$

Based on 100 g of catalyst used, the composition of the catalyst will be as follows:

    Palladium   =   1 g

    SiO$_2$ =   100-1 =   99 g

For 1 g of catalyst

    Palladium required   =   1×(1/100)   =   0.01 g

    Palladium 0.01 g was prepared from Pd(NH$_3$)$_4$Cl$_2$.H$_2$O and molecular weight of Pd is 106.42

the Pd(NH$_3$)$_4$Cl$_2$.H$_2$O (98%)content = $\dfrac{\text{MW of Pd(NH}_3)_4\text{Cl}_2.\text{H}_2\text{O} \times \text{Palladium required}}{\text{MW of Pd} \times 0.98}$

                 =   (263.44/(106.42×0.98))×0.01= 0.0252 g

APPENDIX B

CALCULATION OF THE CRYSTALLITE SIZE

Calculation of the crystallite size by Debye-Scherrer equation

The crystallite size was calculated from the half-height width of the diffraction peak of XRD pattern using the Debye-Scherrer equation.

From Scherrer equation:

$$D = \frac{K\lambda}{\beta \cos \theta}$$ (B.1)

where   D   =   Crystallite size, Å

K =   Crystallite-shape factor = 0.9

λ   =   X-ray wavelength, 1.5418 Å for CuKα

θ   =   Observed peak angle, degree

β   =   X-ray diffraction broadening, radian

The X-ray diffraction broadening (β) is the pure width of a powder diffraction free from all broadening due to the experimental equipment. α-Alumina is used as a standard sample to observe the instrumental broadening since its crystallite size is larger than 2000 Å. The X-ray diffraction broadening (β) can be obtained by using Warren's formula.

From Warren's formula:

$$\beta = \sqrt{B_M^2 - B_S^2}$$ (B.2)

Where B_M =   The measured peak width in radians at half peak height.

B_S =   The corresponding width of the standard material.

Example: Calculation of the crystallite size of Pd/SiO$_2$-SG-im

The half-height width of 111 diffraction peak $=$ 0.89° (from the figure B.1)

$=$ (0.89xπ)/180

$=$ 0.0155 radian

The corresponding half-height width of peak of α-alumina (from the Bs value at the 2θ of 34.08° in figure B.2) $=$ 0.00405 radian

The pure width, β $=$ $\sqrt{B_M^2 - B_S^2}$

$=$ $\sqrt{0.0155^2 \quad 0.00405^2}$

$=$ 0.0151 radian

B $=$ 0.0151 radian

2θ $=$ 33.8°

θ $=$ 16.9°

λ $=$ 1.5418 Å

The crystallite size $=$ $\dfrac{0.9 x 1.5418}{0.0151_{\cos}17.04}$ $=$ 96.04 Å

$=$ 9.6 nm
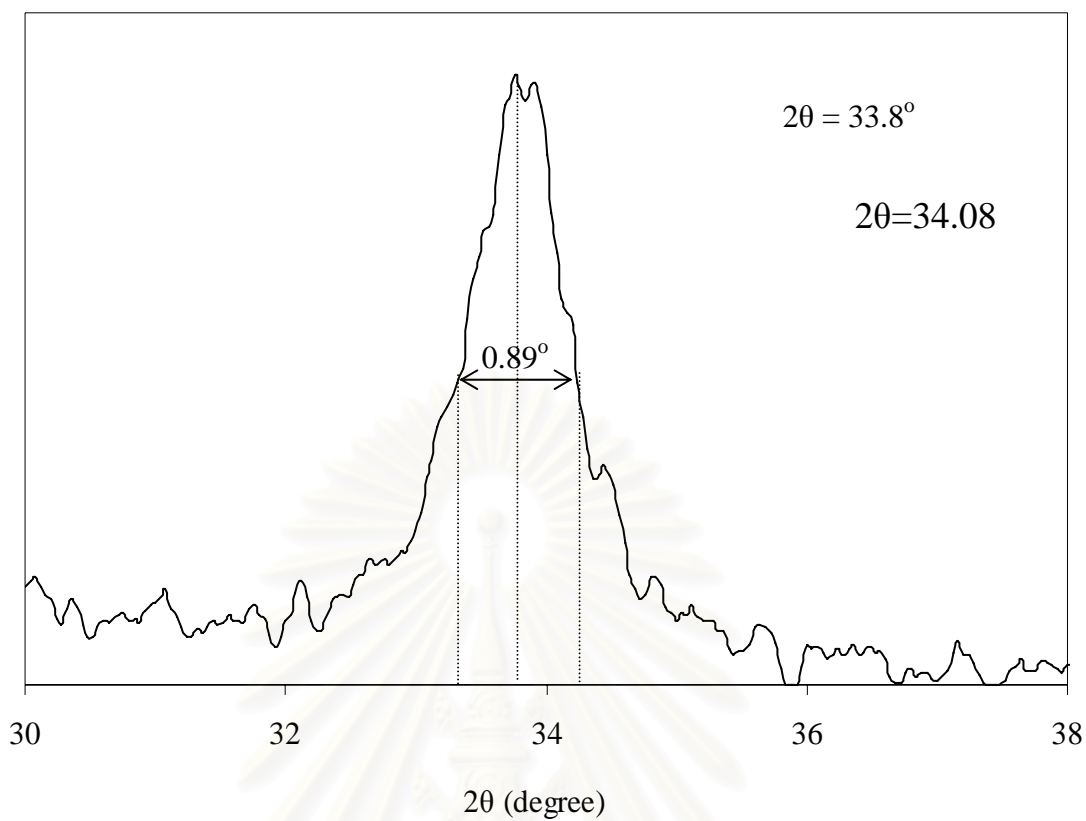
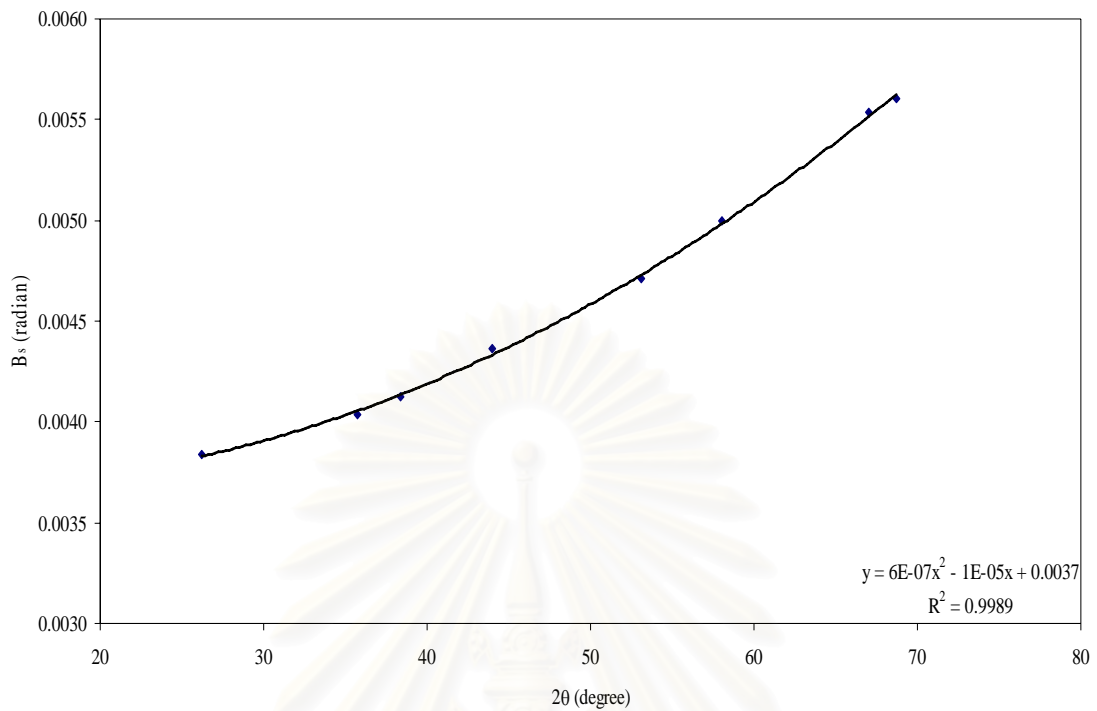Figure B.1 The diffraction peak of Pd/SiO$_2$-SG-im for calculation of the crystallite

size

Figure B.2 The plot indicating the value of line broadening due to the equipment. The

data were obtained by using α-alumina as a standard

APPENDIX C

CALCULATION FOR METAL ACTIVE SITES
AND DISPERSION

Calculation of the metal active sites and metal dispersion of the catalyst measured by CO adsorption is as follows:

Let the weight of catalyst used	= W	g
Integral area of CO peak after adsorption	= A	unit
Integral area of 50 µl of standard CO peak	= B	unit
Amounts of CO adsorbed on catalyst	= B-A	unit
Volume of CO adsorbed on catalyst	= 50×[(B-A)/B]	µl
Volume of 1 mole of CO at 30°C	= 24.86×10^6	µl

Mole of CO adsorbed on catalyst $= [(B-A)/B]×[40/24.86×10^6]$ mole

Molecule of CO adsorbed on catalyst $= [1.61×10^{-6}]× [6.02×10^{23}]×[(B-A)/B]$ molecules

Metal active sites $= 9.68×10^{17}×[(B-A)/B]×[1/W]$ molecules of CO/g of catalyst

Molecules of Pd loaded $= [\%wt\ of\ Pd]×[6.02×10^{23}]/ [MW\ of\ Pd]$ molecules/g of catalyst

Metal dispersion (%) $= 100×[$molecules of Pd from CO adsorption/molecules of Pd loaded$]$

APPENDIX D

CALIBRATION CURVES

This appendix showed the calibration curves for calculation of composition of reactant and products in phenylacetylene hydrogenation. The reactant is phenylacetylene and products are styrene and ethylbenzene.

The flame ionization detector (FID), gas chromatography Shimadzu modal 14B was used for analyzing the concentration of phenylacetylene, styrene and ethylbenzene by using GS-alumina column.

The GS-alumina column was used with a gas chromatography equipped with a flame ionization detector (FID), Shimadzu modal 14B, for analyzing the concentration of phenylacetylene, styrene and ethylbenzene. Conditions uses in GC are illustrated in Table B.1.

Mole of reagent in y-axis and area, which was reported by gas chromatography, in x-axis are exhibited in the curves. The calibration curves of phenylacetylene and styrene

Table D.1 Conditions uses in Shimadzu modal GC-14B.

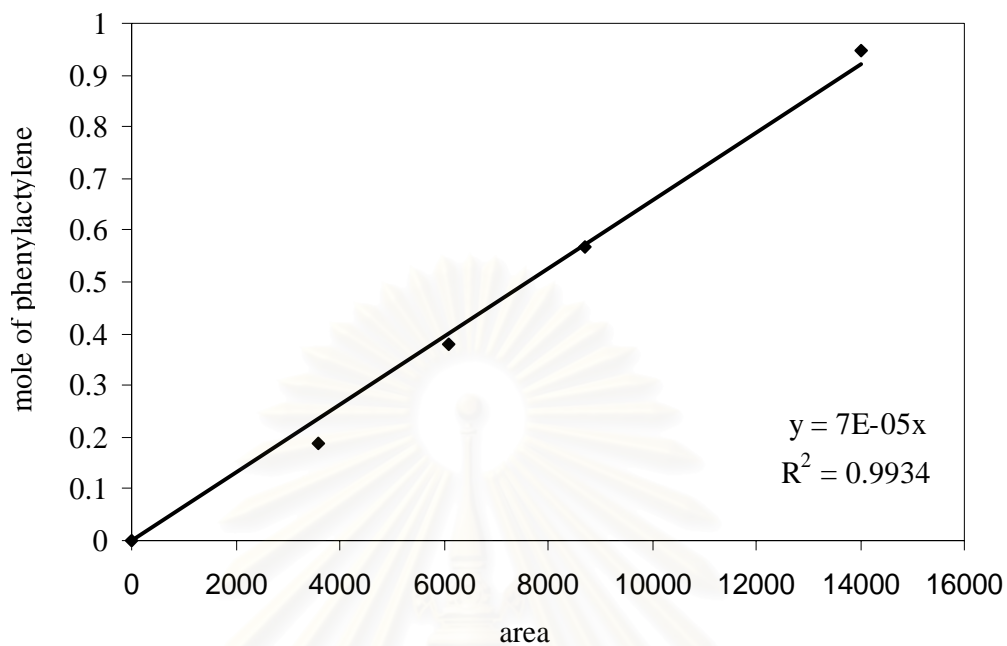| Parameters	Conditions of Shimadzu GC-14B
Width	5
Slope	29
Drift	0
Min. area	100
T.DBL	2.7
Stop time	40
Atten	0
Speed	2
Method	1
Format	1
SPL.WT	100
IS.WT	0

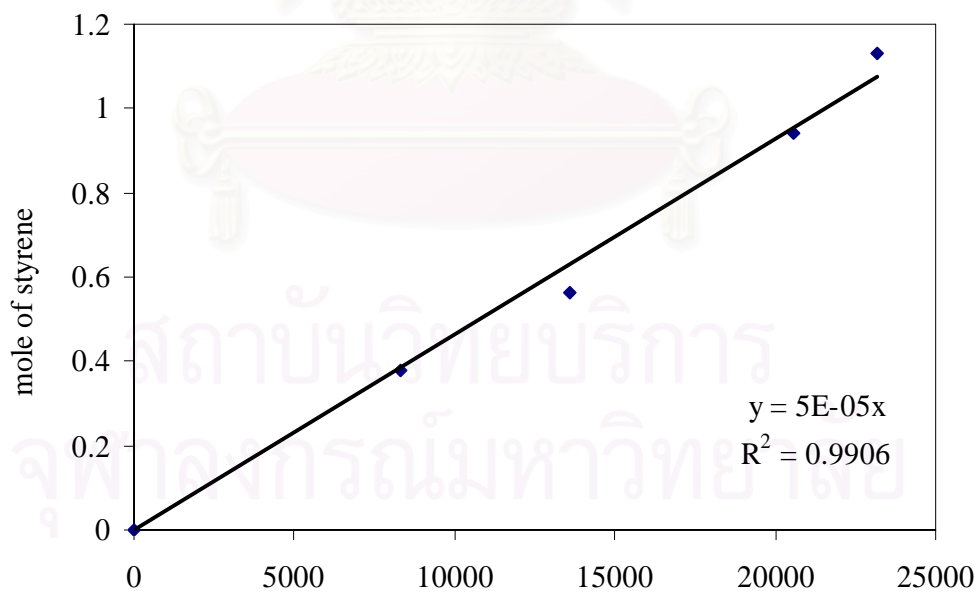Figure D.1 The calibration curve of phenylacetylene

Figure D.2 The calibration curve of styrene

APPENDIX E

CALCULATION OF PHENYLACTYLENE CONVERSION
AND SELECTIVITY

The catalytic performance for the phenylacetylene (PA) hydrogenation was evaluated in terms of activity for phenylacetylene conversion and selectivity.

Activity of the catalyst performed in term of phenylacetylene conversion. Phenylacetylene conversion is defined as moles of phenylacetylene converted with respect to phenylacetylene in feed:

$$\text{PA conversion (\%)} = \frac{\text{mole of PA in feed - mole of PA in product}}{\text{mole of PA in feed}} \times 100 \qquad \text{(E.1)}$$

Where mole of phenylacetylene can be measured employing the calibration curve of phenylacetylene in Figure D.1, Appendix D., i.e.

$$\text{Mole of PA} = (\text{Area of PA peak from integrator plot on GC-14B}) \times 7 \times 10^{-5} \qquad \text{(E.2)}$$

Selectivity of product is defined as mole of styrene (ST) formed with respect to mole of phenylacetylene converted:

$$\text{Selectivity of ST (\%)} = \frac{\text{mole of ST formed}}{\text{mole of total product}} \times 100 \qquad \text{(E.3)}$$

Where mole of styrene can be measured employing the calibration curve of styrene in Figure B.2, Appendix B., i.e.,

$$\text{Mole of styrene} = (\text{Area of styrene peak from integrator plot on GC-14B}) \times 5 \times 10^{-5} \qquad \text{(E.4)}$$

APPENDIX F

CALCULATION OF TURNOVER OF FREQUENCY

Calculation of Turnover frequencies (TOF)

Metal active site $\quad = \quad y \quad$ molecule/g cat.

$$\text{ToF} = \frac{\text{rate}}{(\text{numbers of active site})}$$

$$= \frac{\text{molecule substrate converted}}{[\text{g cat.}]\,[\text{min}]} \left| \frac{[\text{g cat.}]}{y\,[\text{active site}]} \right| \frac{[\text{min}]}{[\text{s}]}$$

$$= \quad [\text{s}^{-1}]$$

APPENDIX G

LIST OF PUBLICATIONS

1. Kunnika Phandinthong, Joongjai Panpranot, Wandee Luesaiwong, and Piyasan Praserthdam, " A Comparative Studyof Liquid Phase Hydrogenation on Ps/SiO_2 in Organic Solvents and Under Pressurized Carbon Dioxide", Proceedings of the Regional Symposium on Chemical Engineering 2005, Hanoi, Vietnam, Nov. 30 – Dec 2, 2005, Ref. No. OCA15.

2. Joongjai Panpranot, Kunnika Phandinthong, Piyasan Praserthdam, Masashi Hasegawa, Shin-ichiro Fujita, and Masahiko Arai, "A Comparative Study of Liquid Phase Hydrogenation on Pd/SiO_2 in Organic Solvents and Under Pressurized Carbon Dioxide: Activity Change and Metal Leaching/Sintering", Journal of Molecular Catalysis A, 2006 (In Press).

VITAE

Miss Kunnika Phandinthong was born in March 10th, 1982 in Bangkok, Thailand. She finished high school from Suksanari School, Bangkok in 2000, and received bachelor's degree in Chemical Engineering from the department of Chemical Engineering, Faculty of Engineering, Chulalongkorn University, Bangkok, Thailand in 2004.